CMOS Monolithic Pixel Sensors based on the Column-Drain Architecture for the HL-LHC Upgrade

K. Moustakas[1], M.Barbero[3], I. Berdalovic[2], C. Bespin[1], P. Breugnon[3], I. Caicedo[1], R. Cardella[2], Y. Degerli[4], N. Egidos Plaja[2], S. Godiot[3], F. Guilloux[4], T. Hemperek[1], T. Hirono[1], H. Krüger[1], T. Kugathasan[2], C. A. Marin Tobon[2], P. Pangaud[3], H.Pernegger[2], P. Riedler[2], P. Rymaszeweski[1], E. J. Schioppa[2], W. Snoeys[2], M. Vandenbroucke[3], T. Wang[1] and N. Wermes[1]

[1]Physikalisches Institut, Bonn University, [2]CERN, [3]CPPM/Aix-Marseille Université, [4]CEA/IRFU

moustakas@physik.uni-bonn.de

ATLAS Phase II Upgrade: ITK

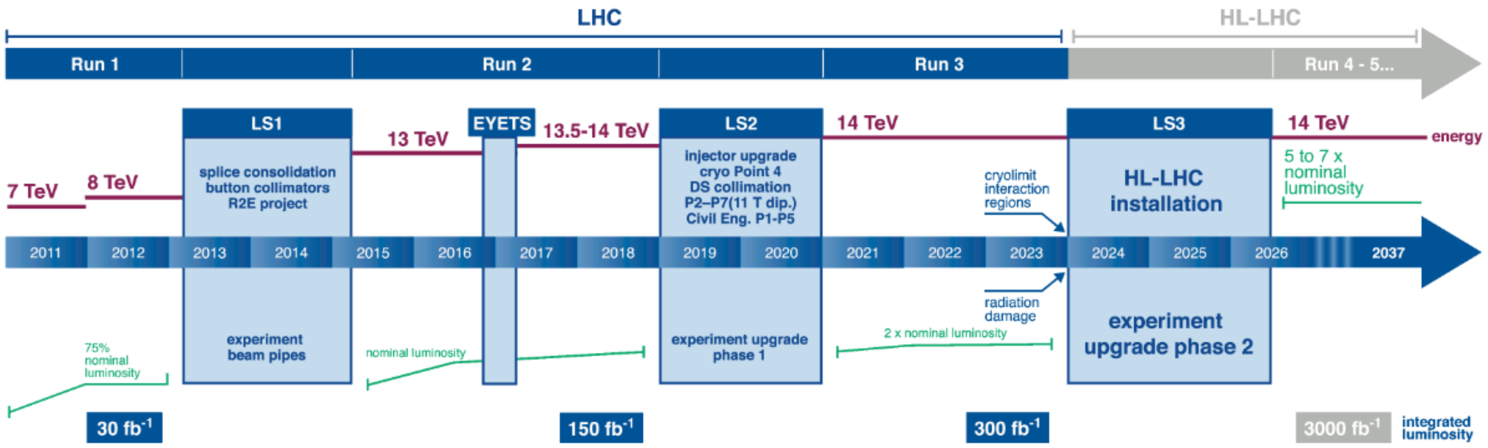

ATLAS-TDR-025, April 2017

	ATLAS-LHC	ATLAS-HL-LHC Outer	ATLAS-HL-LHC Inner
Time resolution [ns]	25		25
Particle Rate [kHz/mm²]	1000	1000	10 000
Fluence [n_{eq}/cm^2]	2×10^{15}	10^{15}	2×10^{16}
Ion. Dose [Mrad]	80	50	> 1000

- A new silicon tracker will be installed during the HL-LHC upgrade in 2025
- Unprecedented requirements for the ATLAS Inner Tracker
  - High radiation level: up to 10^{16} n_{eq}/cm^2, 1Grad TID
  - High particle rate: occupancy, bandwidth

- Depleted Monolithic Active Pixel Sensors (DMAPS) are emerging as a promising alternative for the outer layers
  - Commercial CMOS process
  - No bump bonding, simple assembly

$\left.\right\}$ High Granularity, low material
Low power, low cost

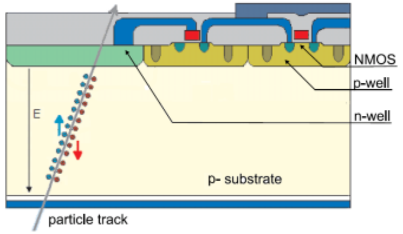

New advancements in imaging CMOS processes: HV/HR

Full depletion $\left(d \sim \sqrt{\rho \cdot V}\right)$

Fast charge collection, high efficiency

DMAPS: Large Vs Small Collection Electrode

Large Collection Electrode – LF-Monopix

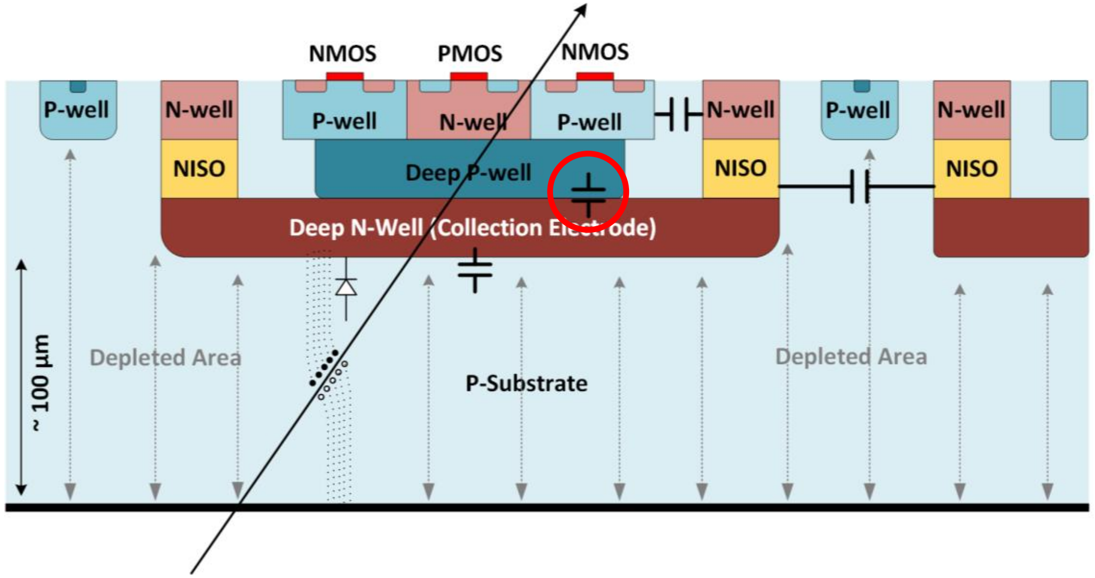

- Large capacitance $C \cong 300 - 400fF$
- Higher analog power, sensitive to crosstalk
- Uniform, strong drift field, high radiation tolerance and detection efficiency

$$\tau_{CSA} \approx \frac{1}{g_m}\frac{C}{C_f}$$

$$ENC^2_{thermal} \approx \frac{4}{3}\frac{kT}{g_m}\frac{C}{\tau_f}$$

Vs

Small Collection Electrode – TJ-Monopix

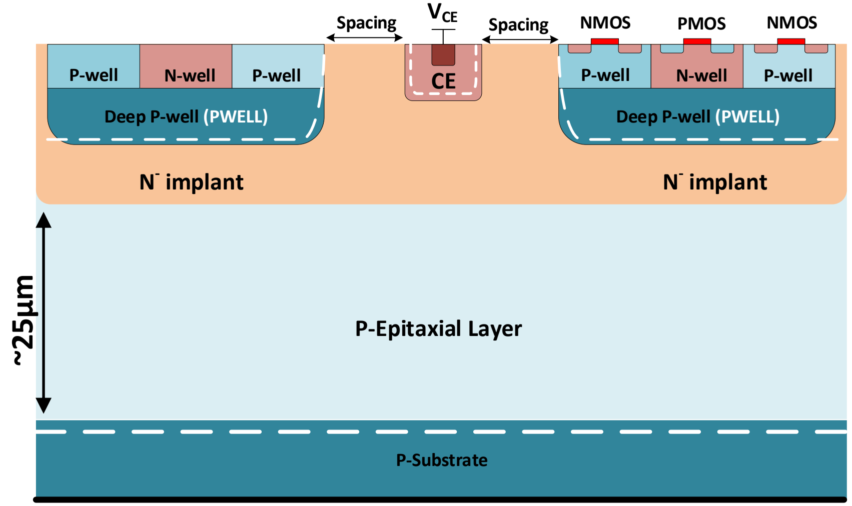

- Small capacitance, $C \cong 3fF \Longrightarrow$ Low Power
- Small pixels (Electrode distance): High granularity
- Less sensitive to crosstalk
- Full depletion can be achieved by modifying the process $\Longrightarrow$ radiation tolerance increase

$$\frac{S}{N} \approx \frac{Q/C}{\sqrt{g_m}} \sim \frac{Q/C}{\sqrt[m]{P}} \Longrightarrow P \sim \left(\frac{Q}{C}\right)^{-m}$$

Small Collection Electrode – Modified process

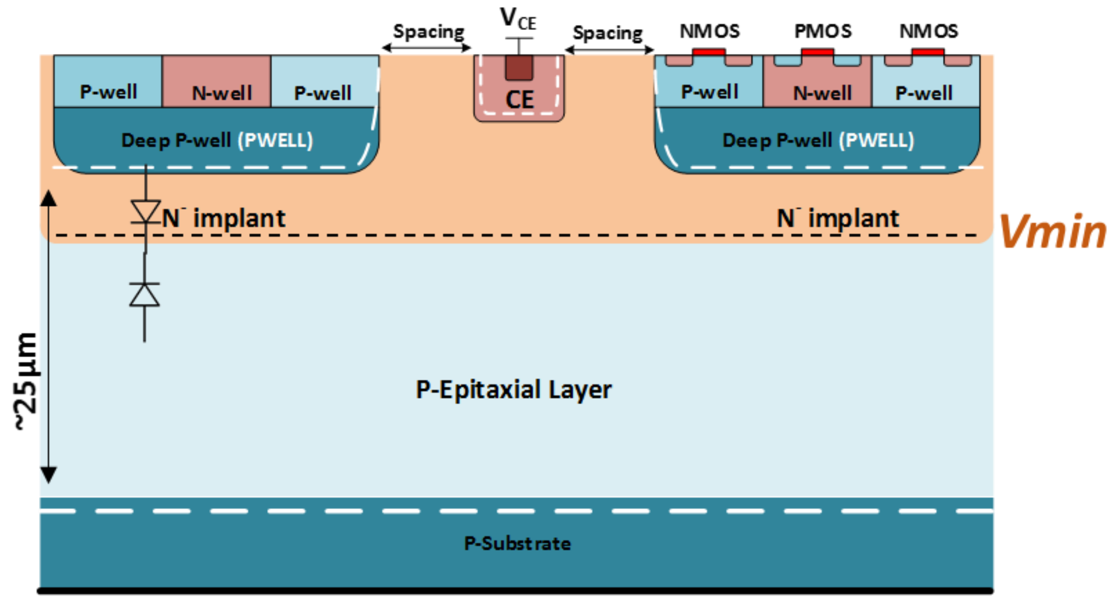

W.Snoeys, doi.org/10.1016/j.nima.2017.07.046

- Commercial 180nm CMOS imaging process
- High resistivity p-epitaxial substrate (>1KΩ·cm)
- Process modification (CERN & foundry): Implantation of an n-type planar layer
- Two opposite pn-junctions are formed that fully deplete the sensing volume
- A potential minimum is formed that enhances charge collection under the deep p-well

- Reduced charge sharing
- Charge collection time is enhanced and spread is reduced
- No significant performance degradation after irradiation

H. Pernegger et al., DOI 10.1088/1748-0221/12/06/P06008

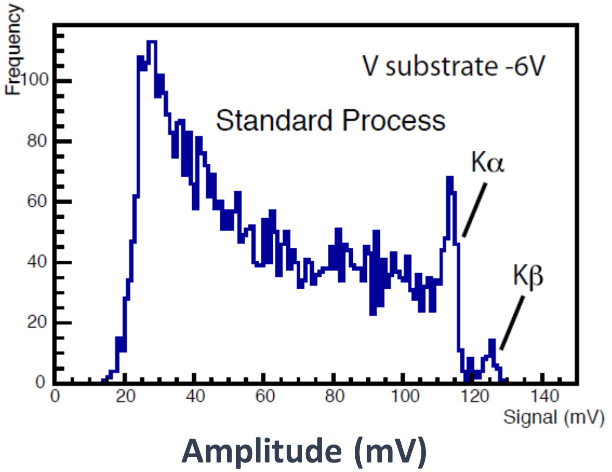

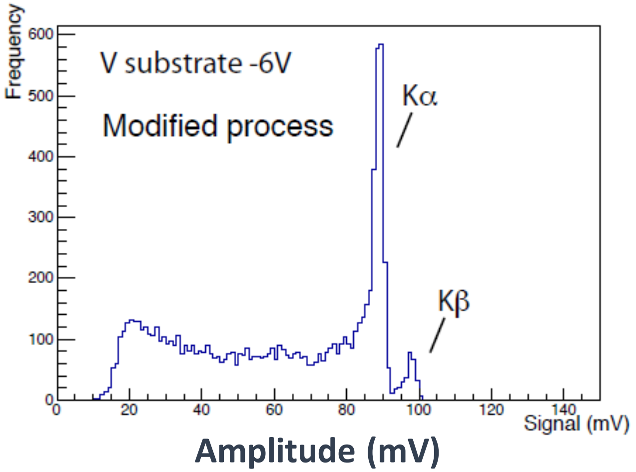

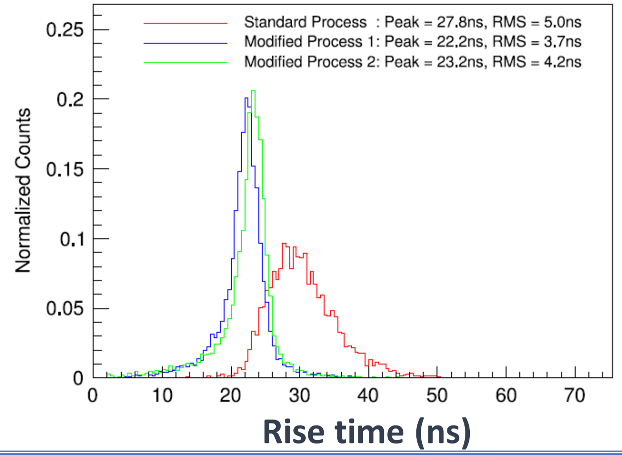

Column-Drain Readout Architecture

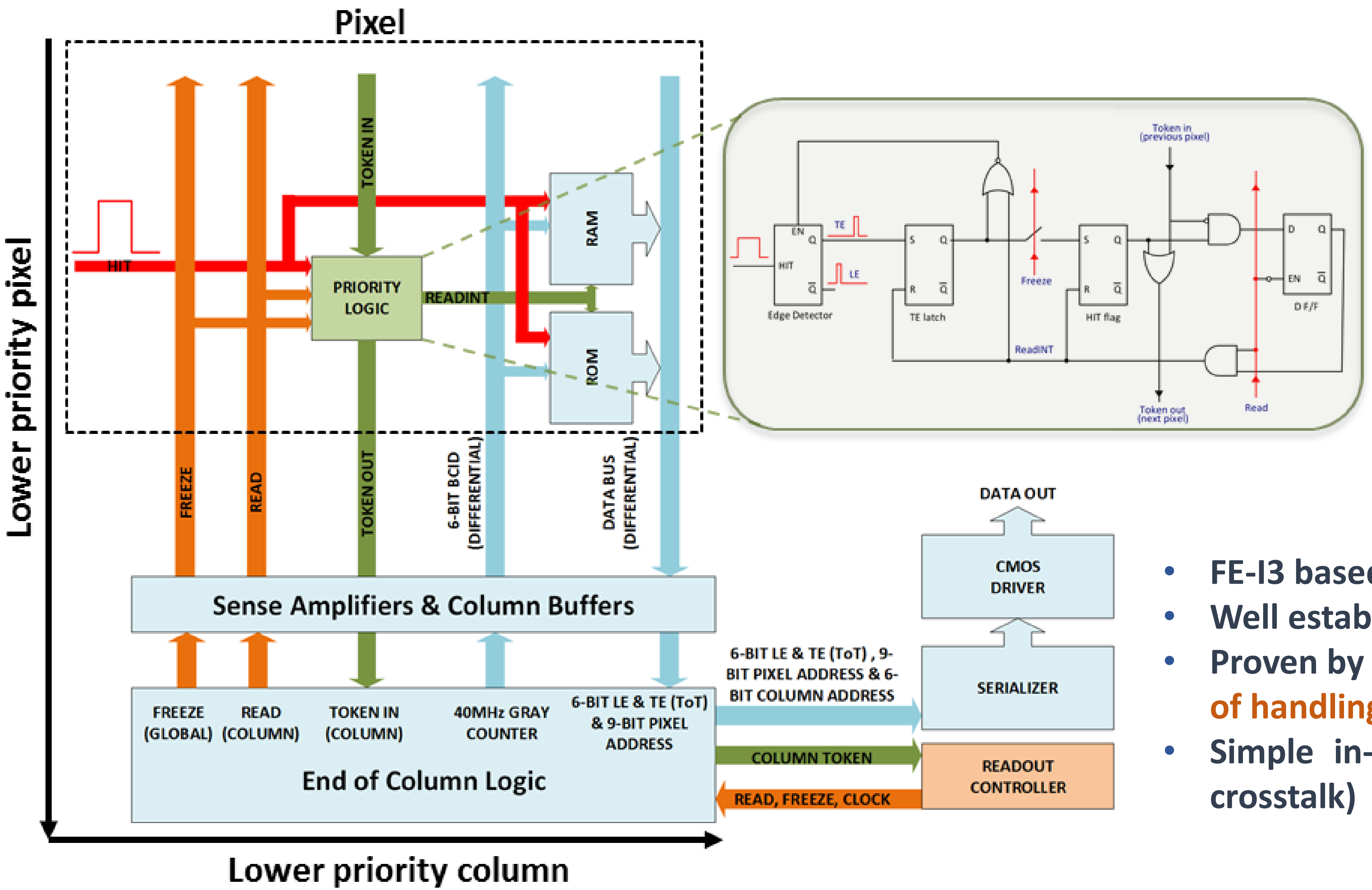

- FE-I3 based approach (pixel priority arbitration)
- Well established capabilities (b-layer)
- Proven by architecture simulation to be capable of handling the hit rate of the ITK outer layers
- Simple in-pixel logic (small pixels & reduced crosstalk)

Column-Drain Readout Architecture

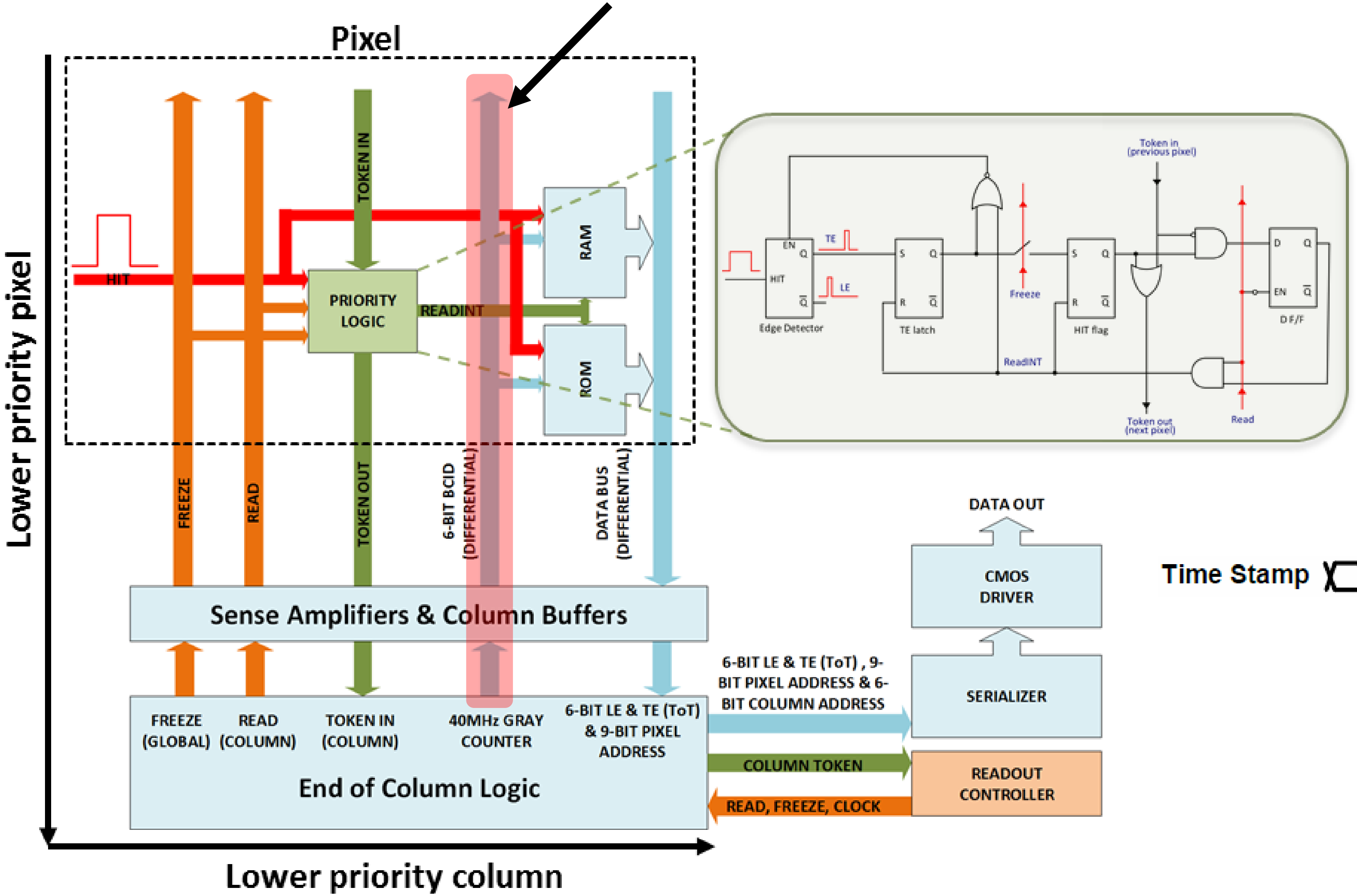

1. **Time stamp is distributed in the matrix**

Column-Drain Readout Architecture

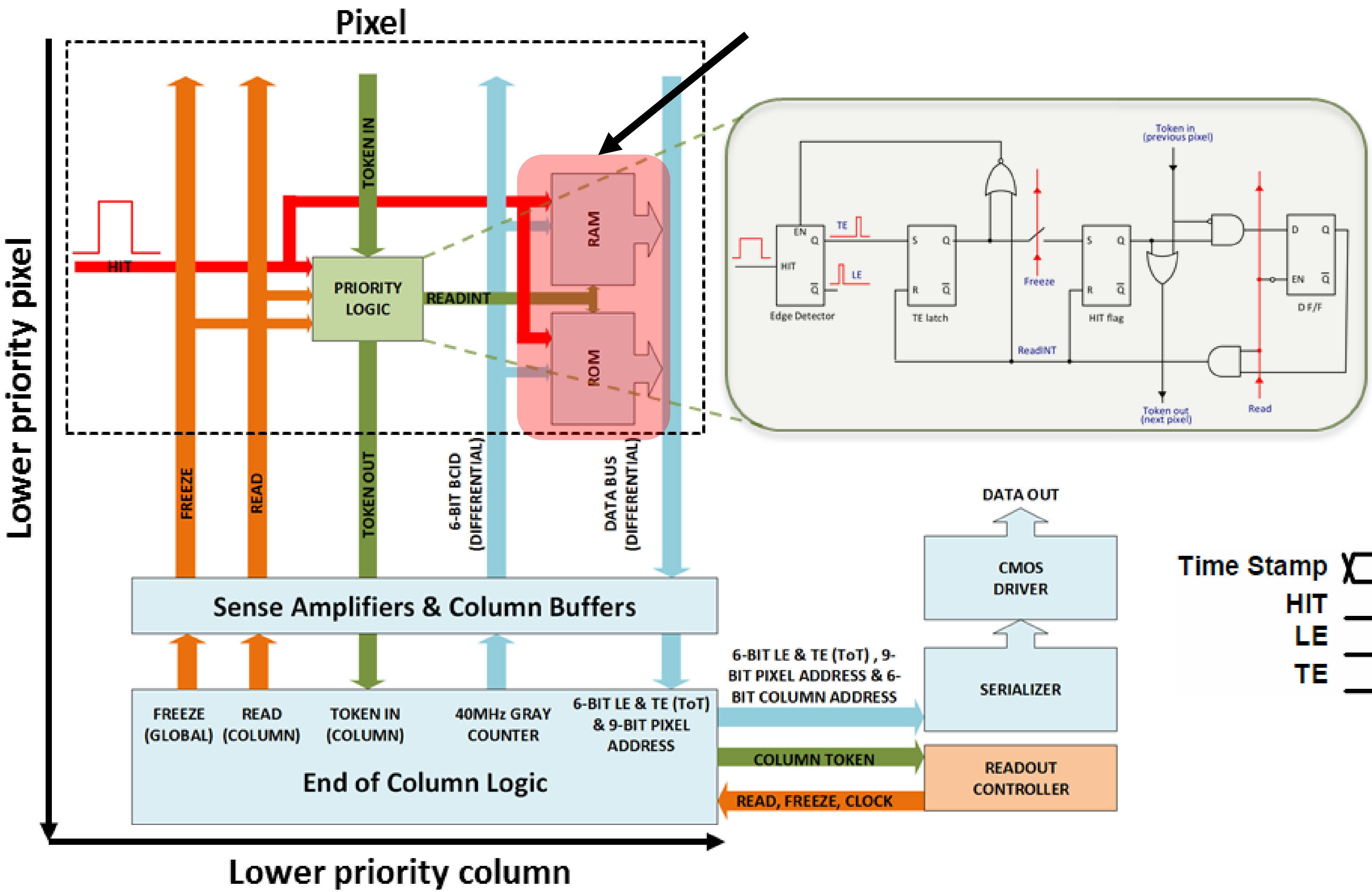

1. Time stamp is distributed in the matrix
2. Hit information (timing & ToT) stored in the pixel

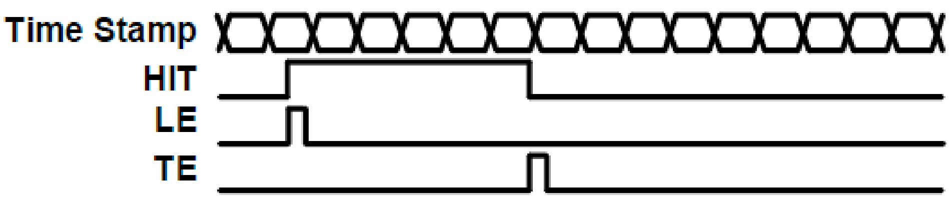

Column-Drain Readout Architecture

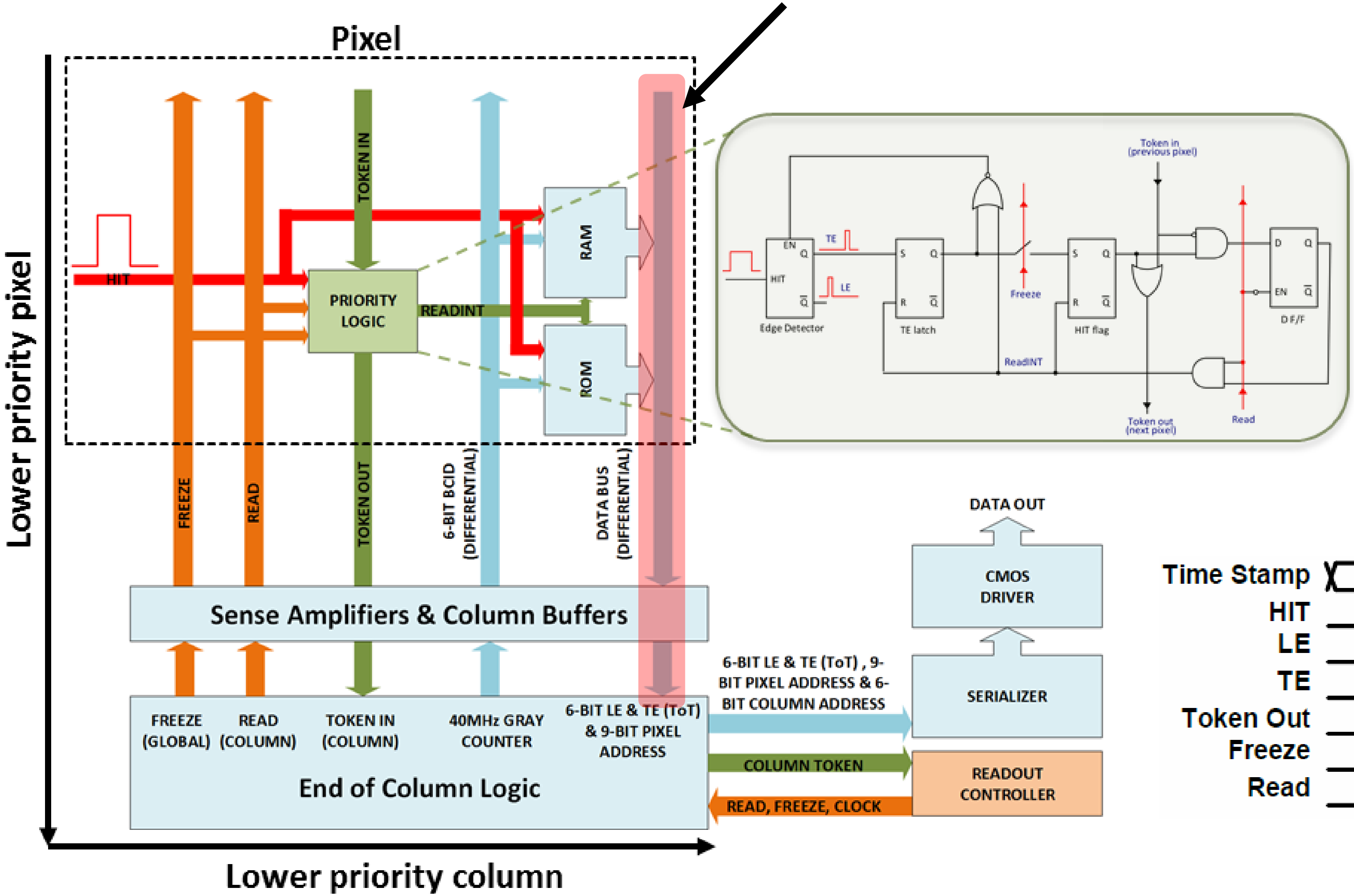

1. Time stamp is distributed in the matrix
2. Hit information (timing & ToT) stored in the pixel
3. Readout initiated by a token. Priority arbitration over the shared bus

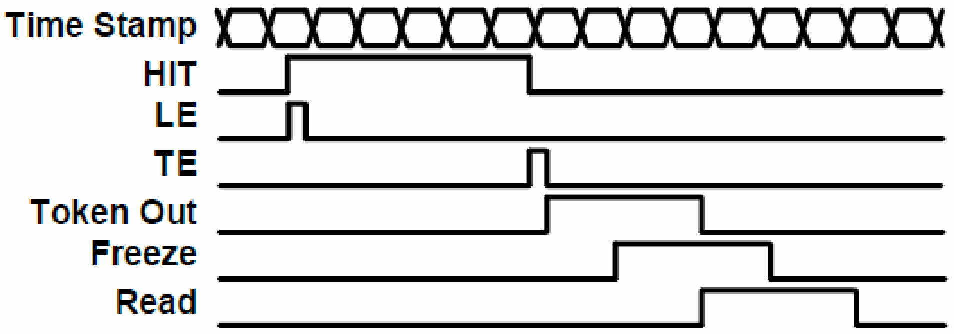

Large-Scale Demonstrators

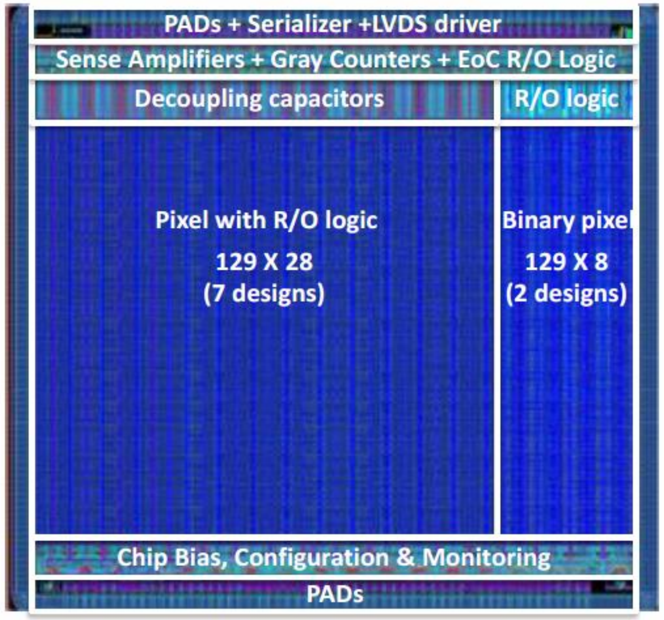

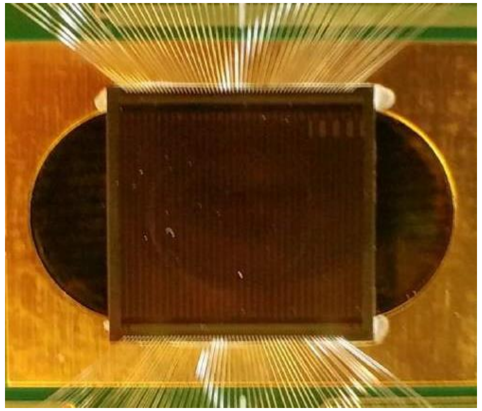

A) Large collection electrode: LF-Monopix (Bonn, CPPM, IRFU)

- 129x36 pixel matrix, 50x250μm^2 pixel size, 10x9.5mm^2 chip size
- Synchronous column-drain readout architecture, 8-bit ToT resolution
- ≅300mW/cm^2 analog power consumption
- High breakdown voltage (-280V)
- 2500 e$^-$ threshold with 100e- dispersion (can be tuned to 1500e$^-$ with noise tuning)
- 120-240 e$^-$ ENC with 30-70 e- dispersion (flavor dependent)
- 10-12μV/e$^-$ gain

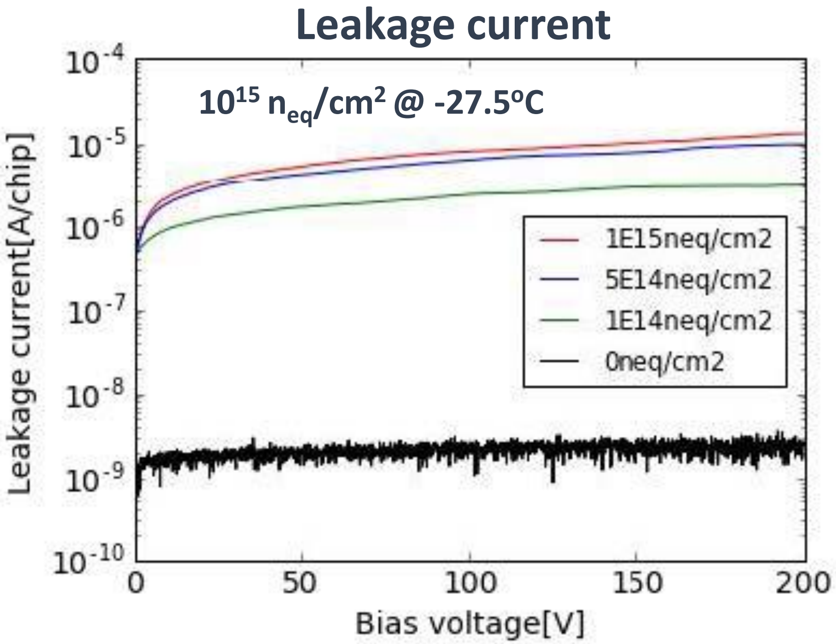

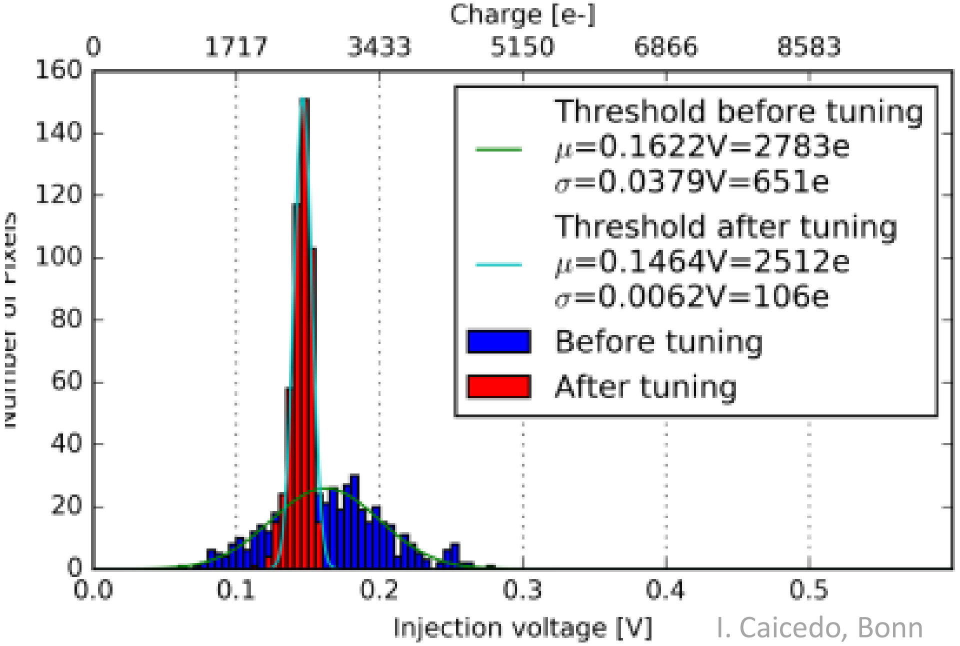

I. Caicedo, Bonn

Large-Scale Demonstrators

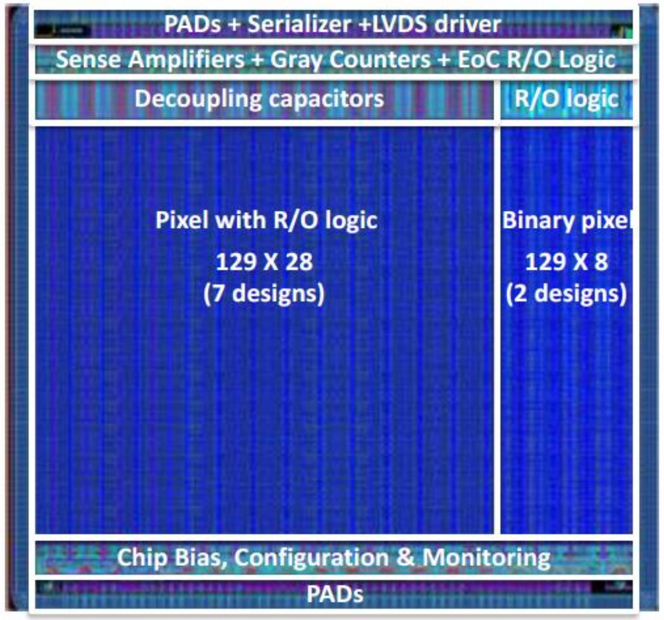

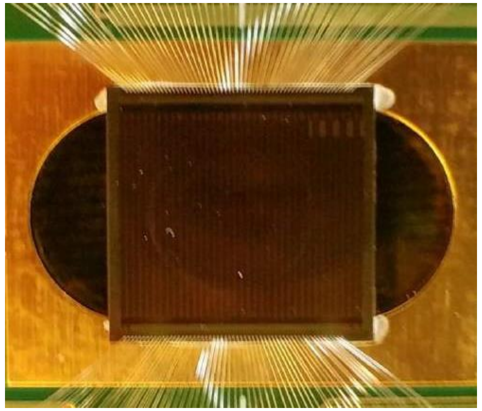

A) Large collection electrode: LF-Monopix (Bonn, CPPM, IRFU)

- Breakdown voltage remains high (<-200 V) after irradiation to 10^{15} n_{eq}/cm^2
- No loss in gain after irradiation to 10^{15} n_{eq}/cm^2
- ENC increases by 150e- due to ≅1Mrad background TID
- High detection efficiency (98,9%) even after irradiation up to $10^{15} n_{eq}/cm^2$ with noise occupancy << 10^{-6} hits/BX

Gain and noise

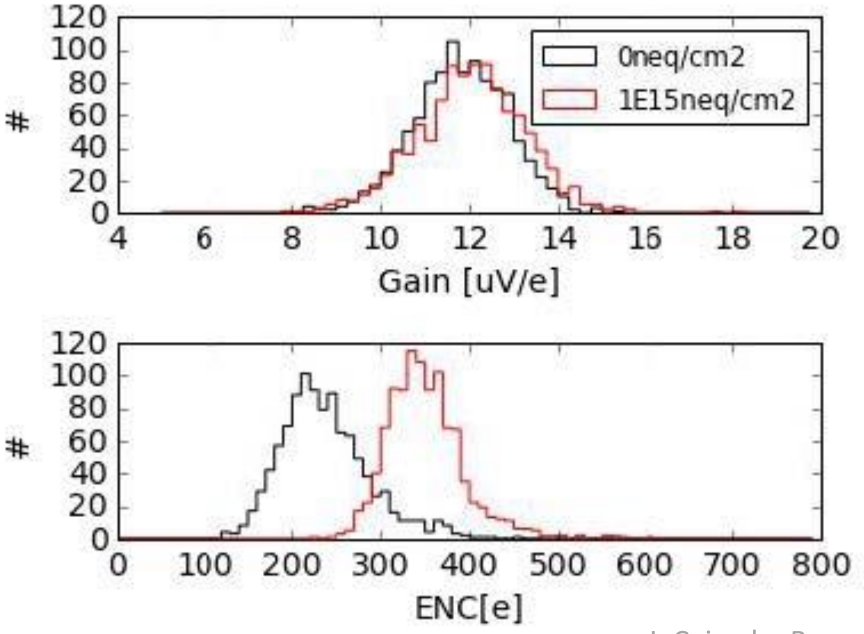

I. Caicedo, Bonn

Efficiency after irradiation 10^{15} n_{eq}/cm^2

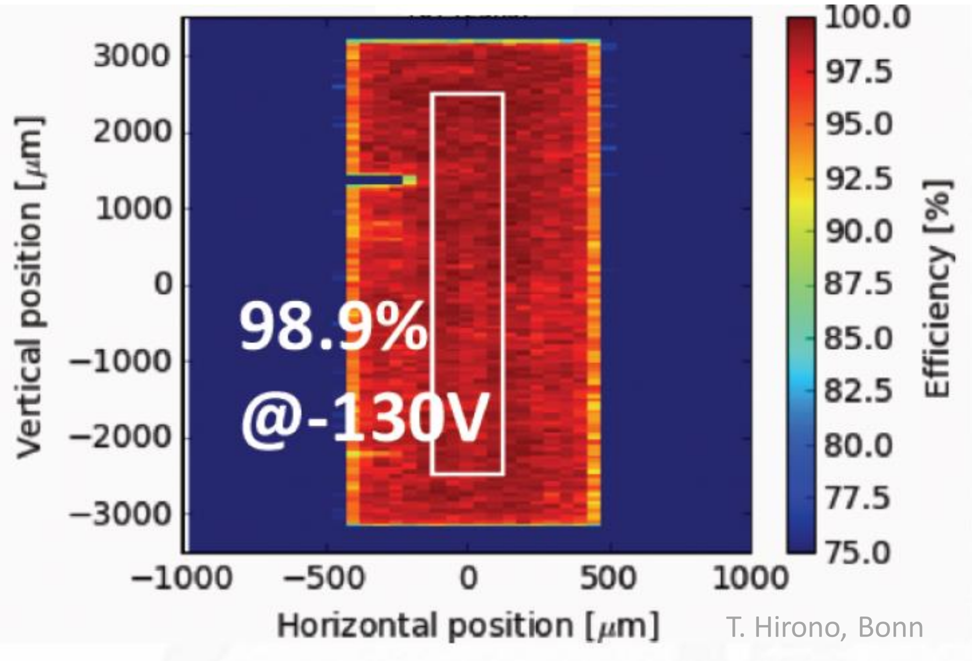

T. Hirono, Bonn

Large-Scale Demonstrators

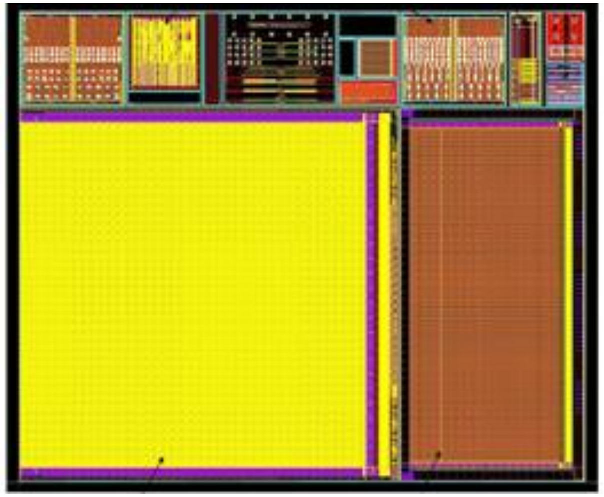

B) Small collection electrode: TJ-Monopix, MALTA (CERN, Bonn)

- Encouraging results show that the modified process sensor enables increased radiation tolerance combined with very small sensor capacitance
- Enables the design of an optimized, low noise & low power analog front end
- *Design of two large-scale demonstrator DMAPS, with integrated in-pixel readout logic, to meet the ALTAS ITK outer layer specifications*

MALTA: $2x2cm^2$

- Novel asynchronous readout architecture
- Time-walk based charge information
- Standard pixels with different reset mechanisms
- Analog output voltage clipping

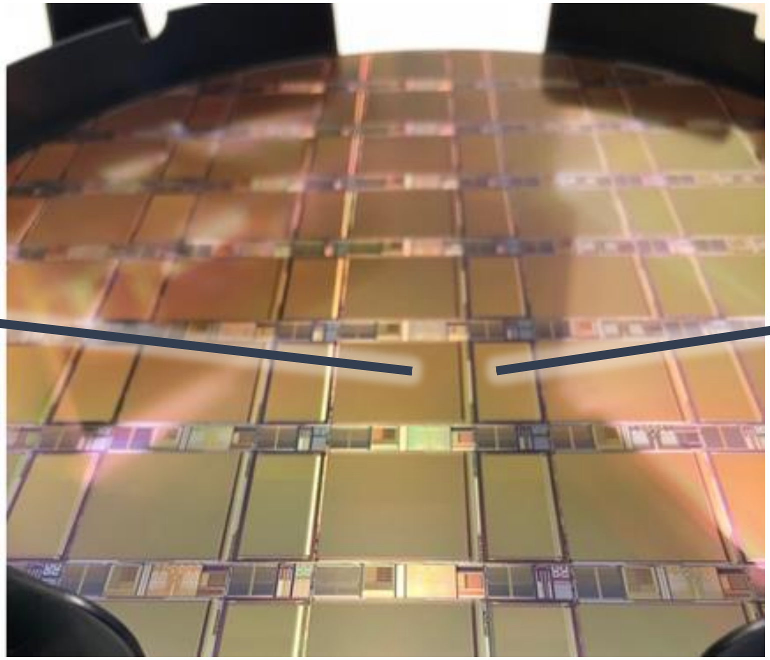

TJ-Monopix: $1x2cm^2$

- Synchronous column – drain readout architecture
- 6-bit ToT information
- Standard pixels with PMOS reset
- Leakage compensation pixels
- Frontside biased AC coupled pixels

Low Power Optimized Front End

- For a typical input charge close to the MPV (1250e⁻):

$$V_{in} = \frac{e^- q_e}{C} \cong \frac{0,2fC}{3fF} \cong 65mV$$

- Design motivation: To take advantage of the high input voltage, a voltage amplifier can take the place of a standard CSA and can be optimized for minimal power consumption and fast timing response

- The analog output node is stabilized at low frequencies by active feedback using M1
- M3 acts as a source follower to avoid loading the input node (IN)
- M4 is a cascode device to increase the gain at the high impedance output node (OUTA)
- Efficient current usage (the same branch current powers the source follower and the amplification stage)

Amplifier

Operating principle derived from the ALPIDE detector

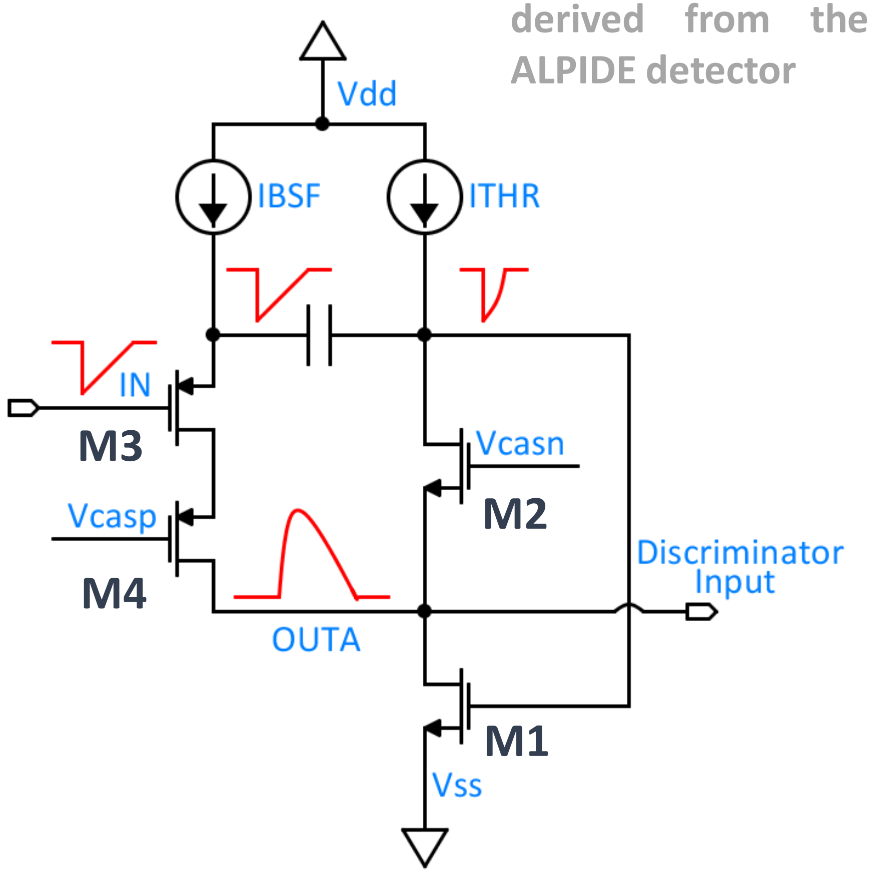

$$Gain = \frac{V_{OUTA}}{Q_{IN}} \cong 0.4\, {}^{mV}/_{e^-}$$

$$ENC \cong 12e^-$$
$$Threshold \cong 300e^-$$

$$Power = 0.9\mu W$$

Low Power Optimized Front End

- **Simple discriminator** design due to the high gain
- Two options for the sensor baseline reset, diode or PMOS device
- **Enclosed layout** of critical transistors for **increased TID tolerance**

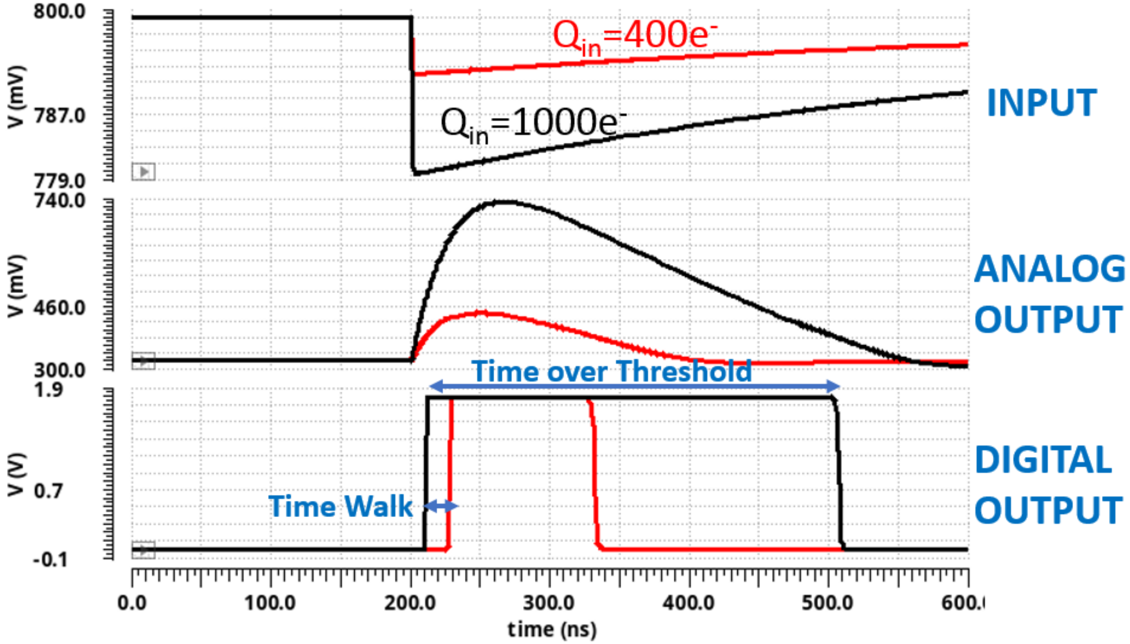

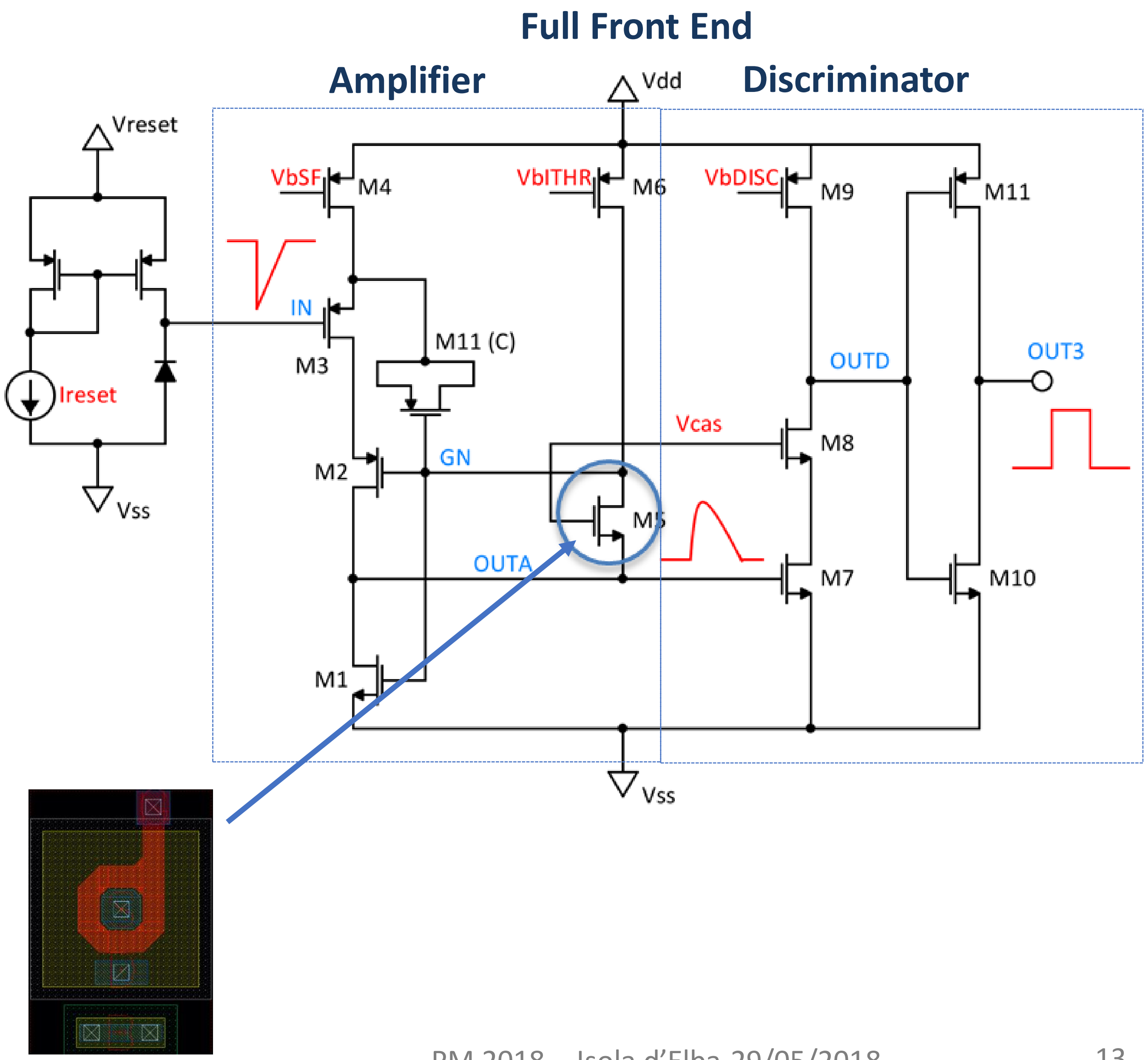

TJ-Monopix Chip Design

2x2 Pixel Layout

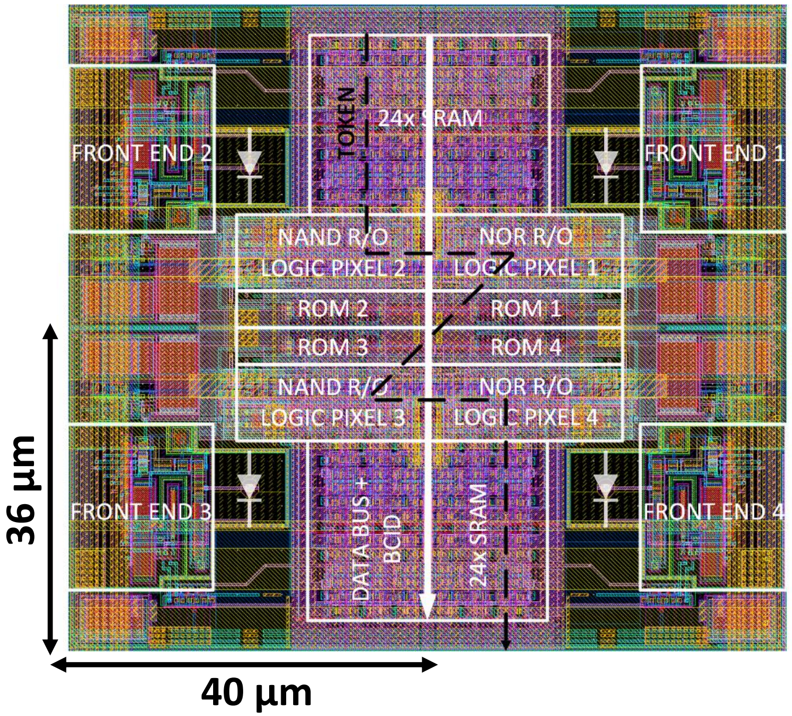

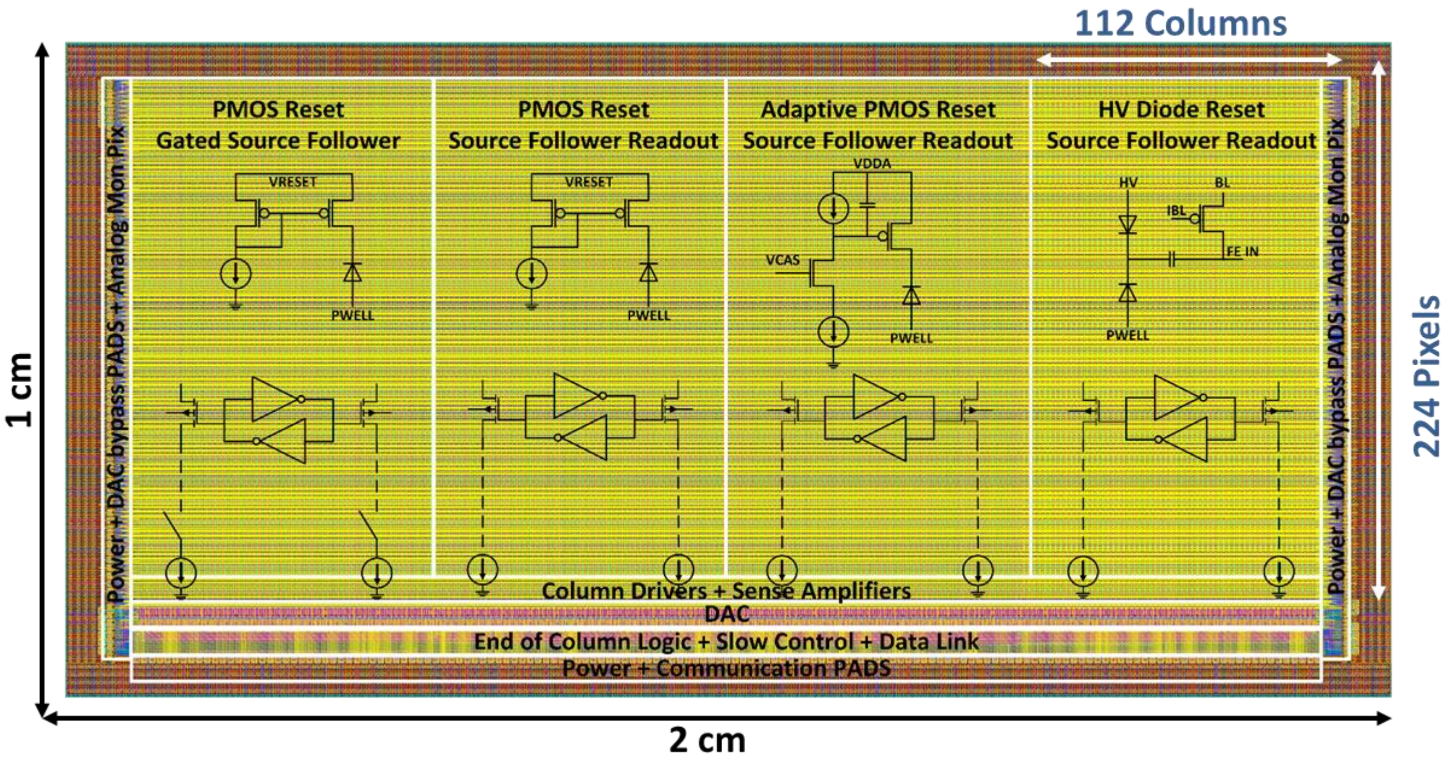

- **Small pixel size:** 36x40 µm²
- **Low power:** $< 65\ mW/cm^2$
- **Low threshold dispersion**, no in-pixel tuning
- Design and layout strategies to minimize crosstalk

- **1x2cm²** size, **224x448** pixel matrix
- **4 Flavors,** Individual readout per flavor
  1. Improved low power column bus readout
  2. Standard PMOS input reset
  3. Adaptive input reset (Leakage compensation)
  4. Frontside HV biased AC coupled pixels

TJ-Monopix Measurement Results

2nd flavor: PMOS reset I) PWELL=-5V, PSUB=-20V

- Injection scan of the whole flavor with reverse bias applied
- PWELL mainly influences the detector capacitance, PSUB the bulk depletion
- Different deep p-well coverage across the column, to test the effect on depletion and charge collection

S-Curve Superposition (Histogram)

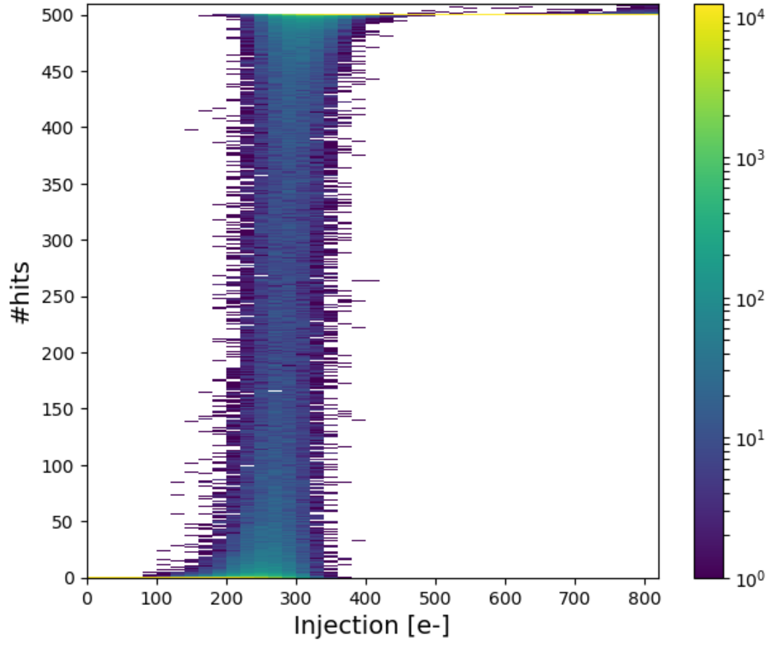

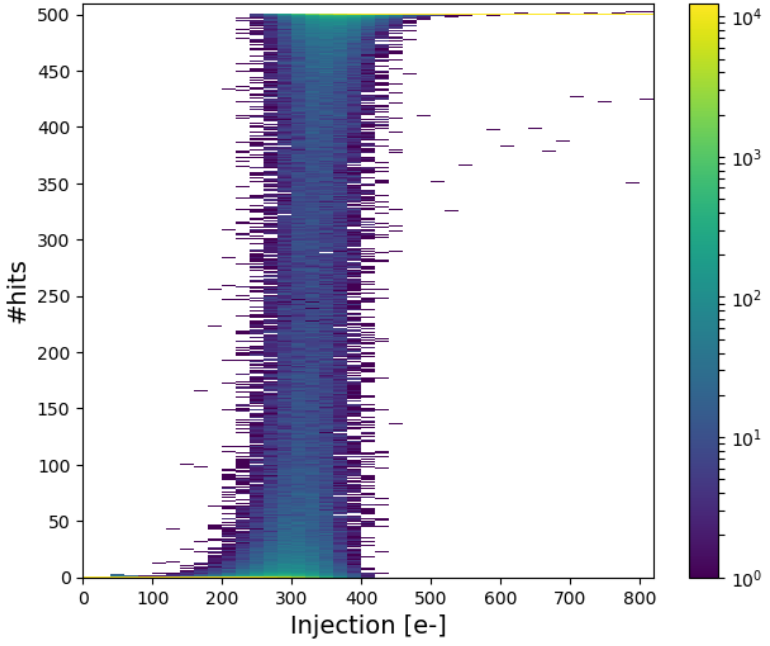

REM DPW – top half of each column (112 pixels)

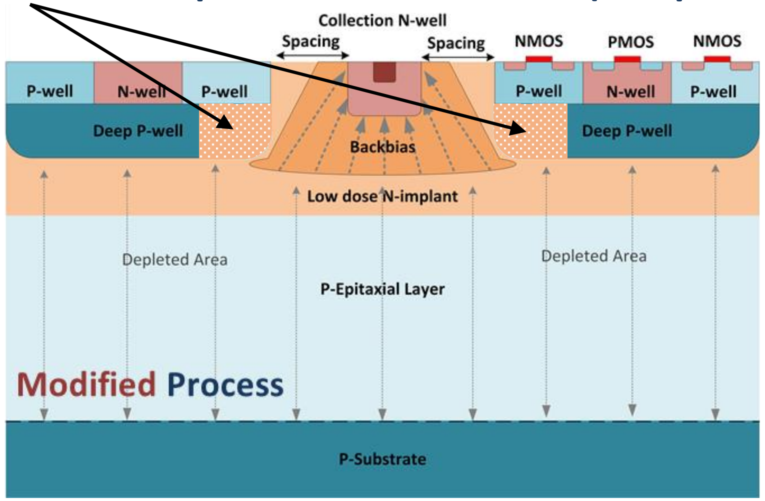

FULL DPW – bot half of each column (112 pixels)

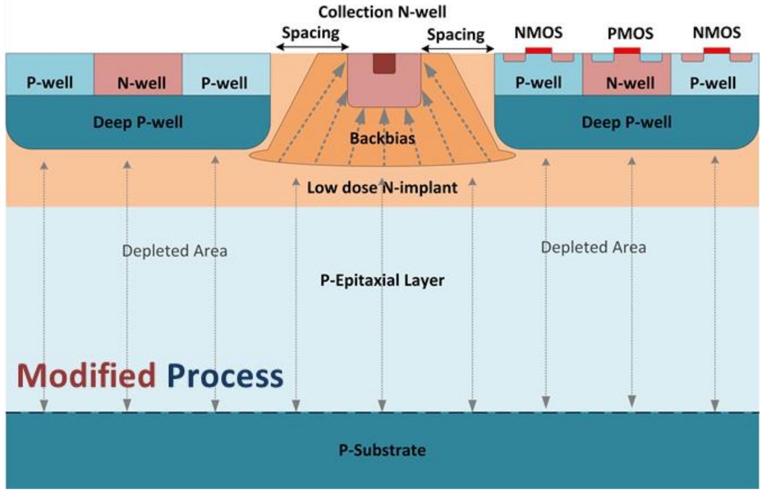

2nd flavor: PMOS reset I) PWELL=-5V, PSUB=-20V

- Threshold mean ≅ 270e⁻, total dispersion ≅ 31e⁻. The dispersion of the front-end is less due to the added dispersion of the small injection capacitance
- Higher threshold and dispersion for the removed DPW region (lower input signal)
- ENC mean ≅ 11e⁻, dispersion ≅ 0.8 e⁻. (In agreement with simulation)

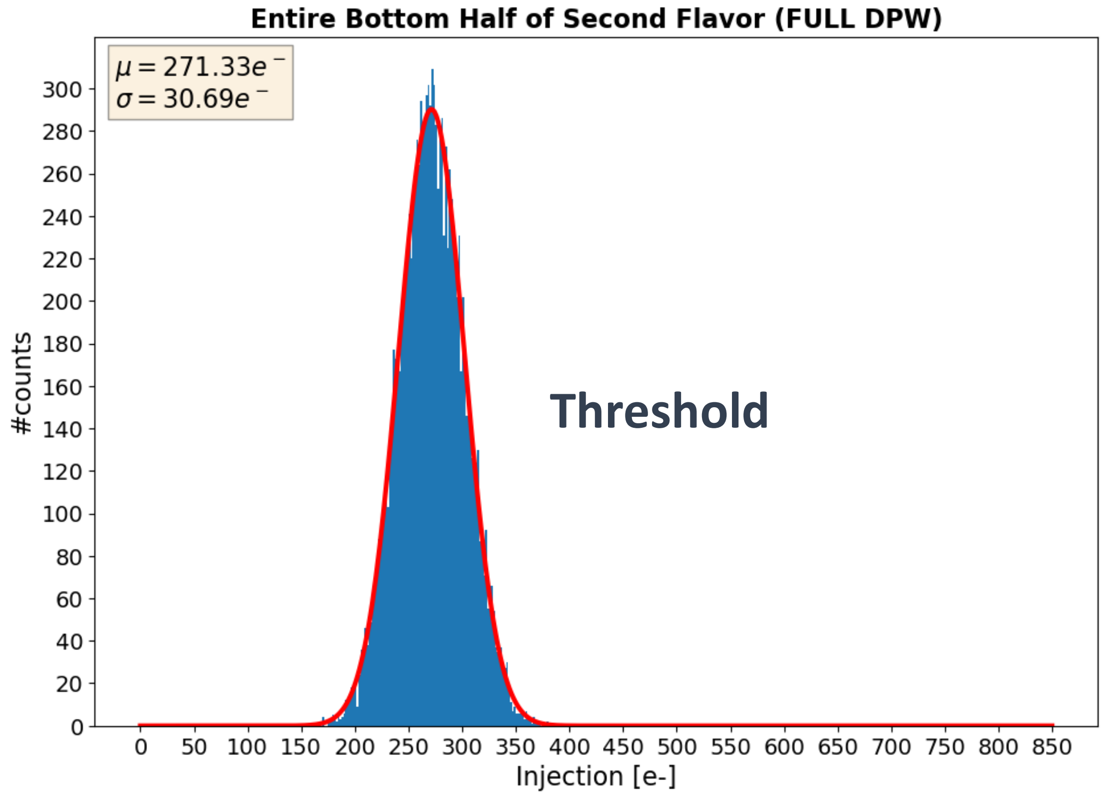

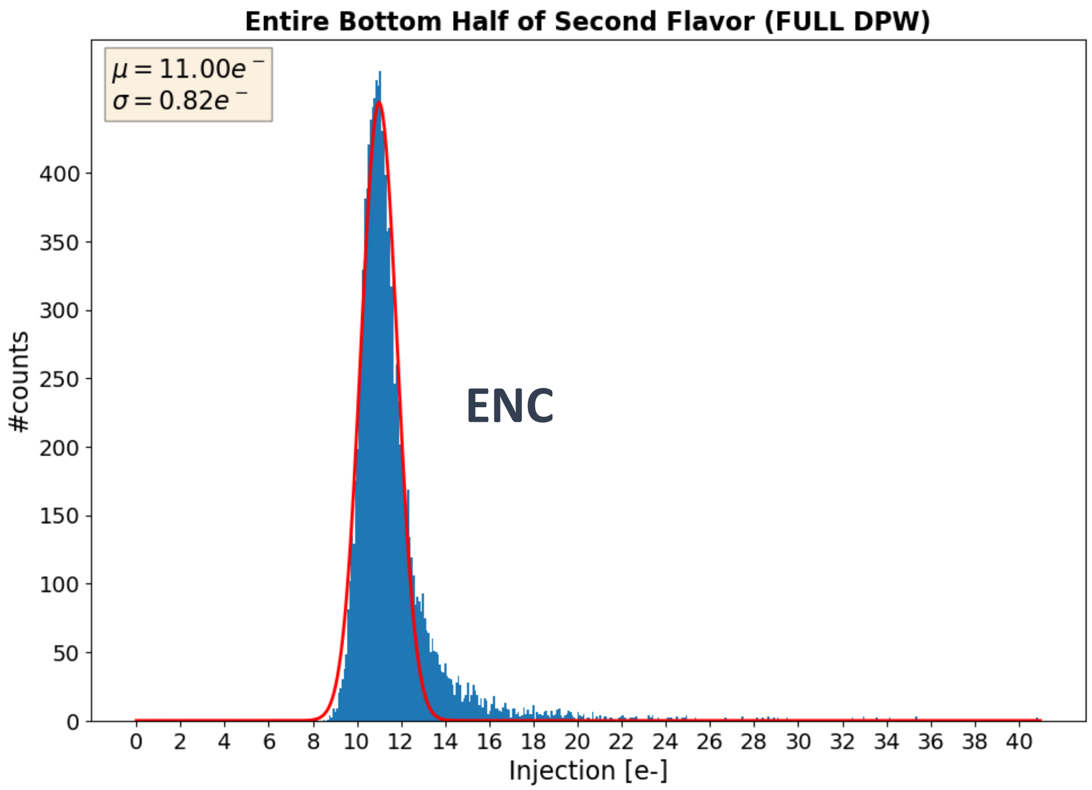

TJ-Monopix Measurement Results

- ^{55}FE spectrum of two different flavors using the analog output of special analog monitoring pixels
- Cleary visible Kα and Kβ peaks
- Higher amplitude for the HV flavor due to the higher saturation input voltage
- FWHM ≅ 55e$^-$, **ENC≅19e$^-$** (after subtraction of the Fano noise)

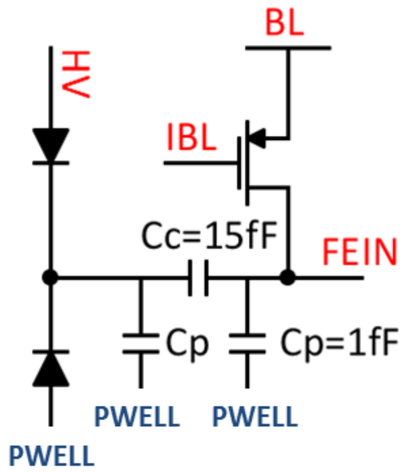

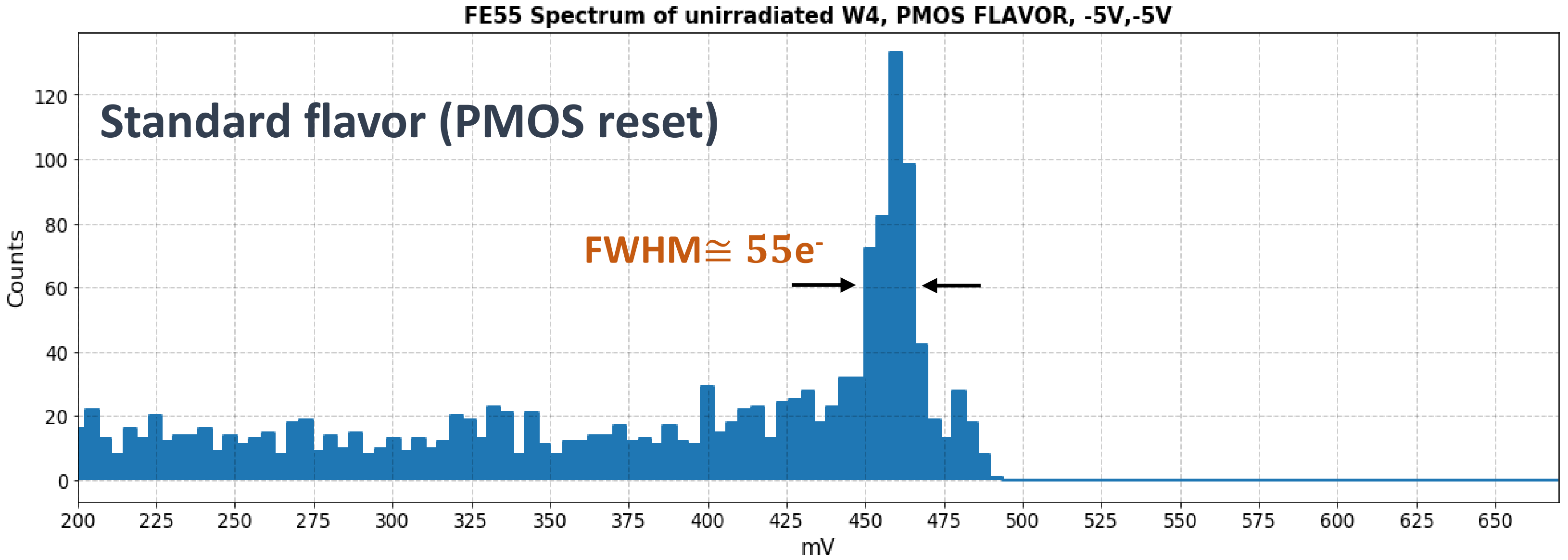

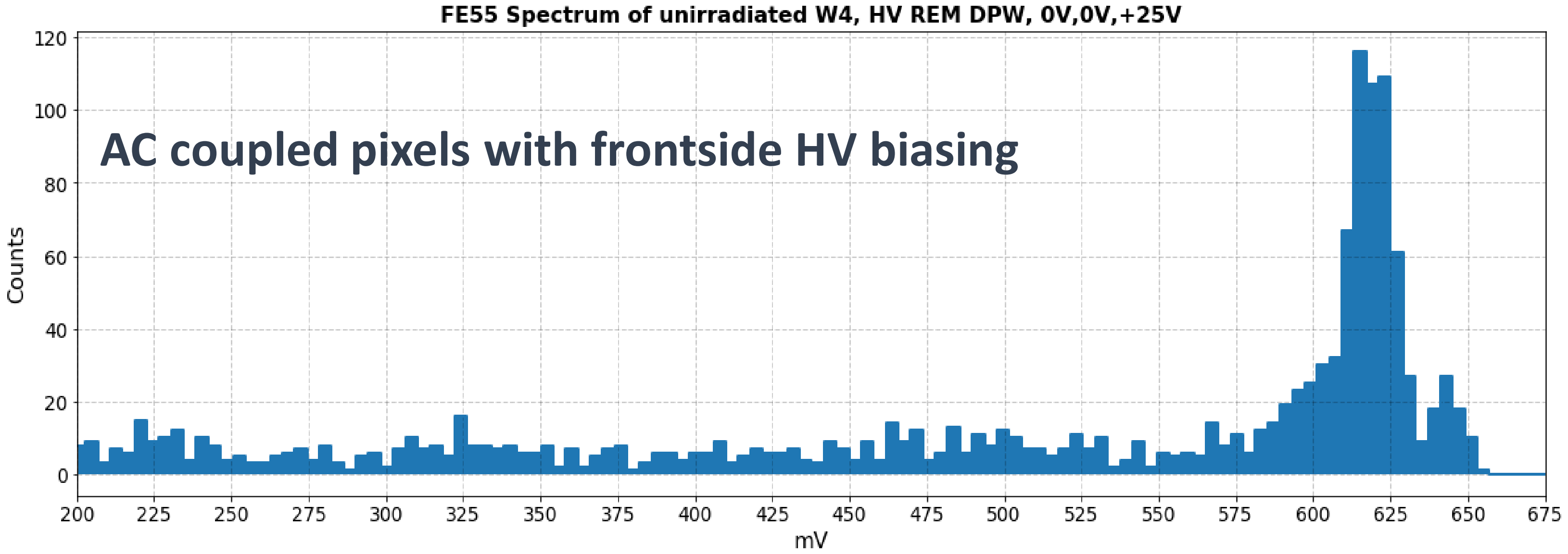

TJ-Monopix Measurement Results

- TJ-Monopix chips were irradiated up to to 10^{15} n_{eq}/cm^2, and are fully **functional**
- ^{55}FE spectrum of the HV AC coupled flavor for irradiated and unirradiated samples was acquired using the full digital readout (6-bit ToT information)
- The Kα peak voltage is lower due to the different front end settings that were applied because of the increased noise after irradiation (higher threshold)

^{55}FE spectrum

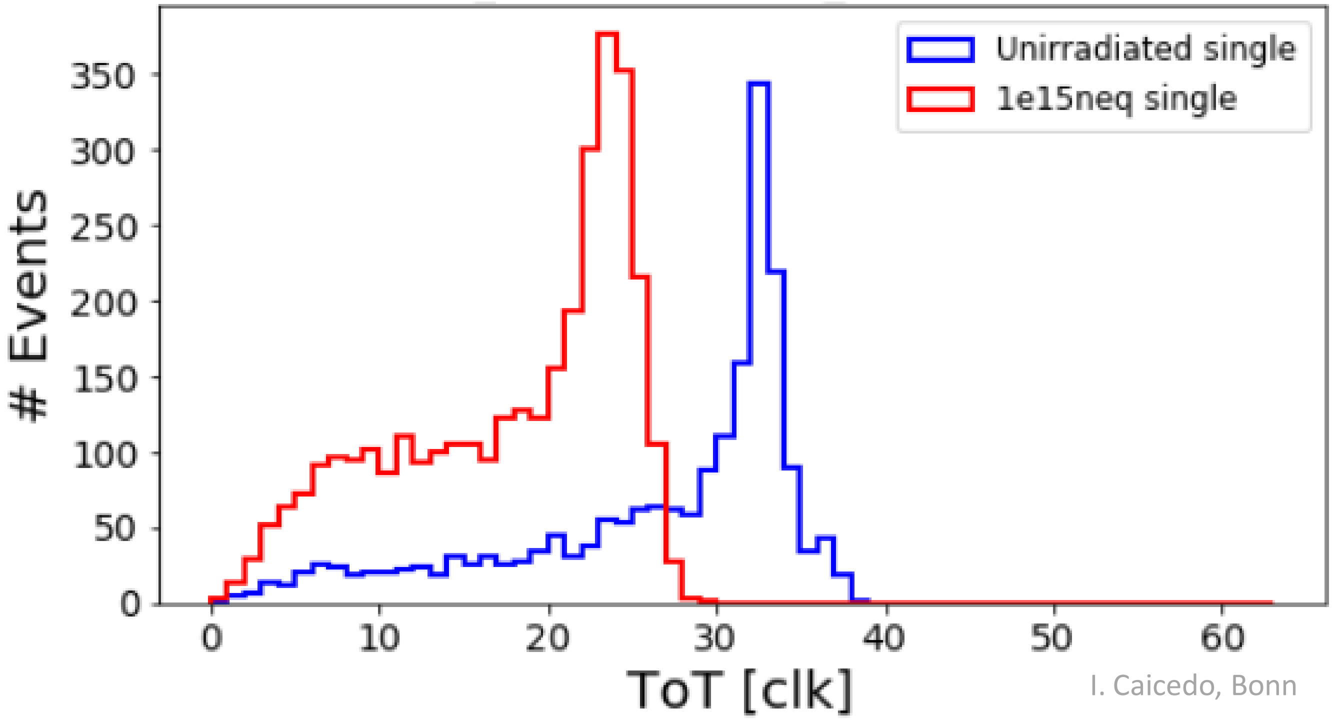

I. Caicedo, Bonn

MALTA measurement results

- Timing response to ^{90}Sr source
- Most of the hits are in-time
- Hits outside in-time region are shared hits

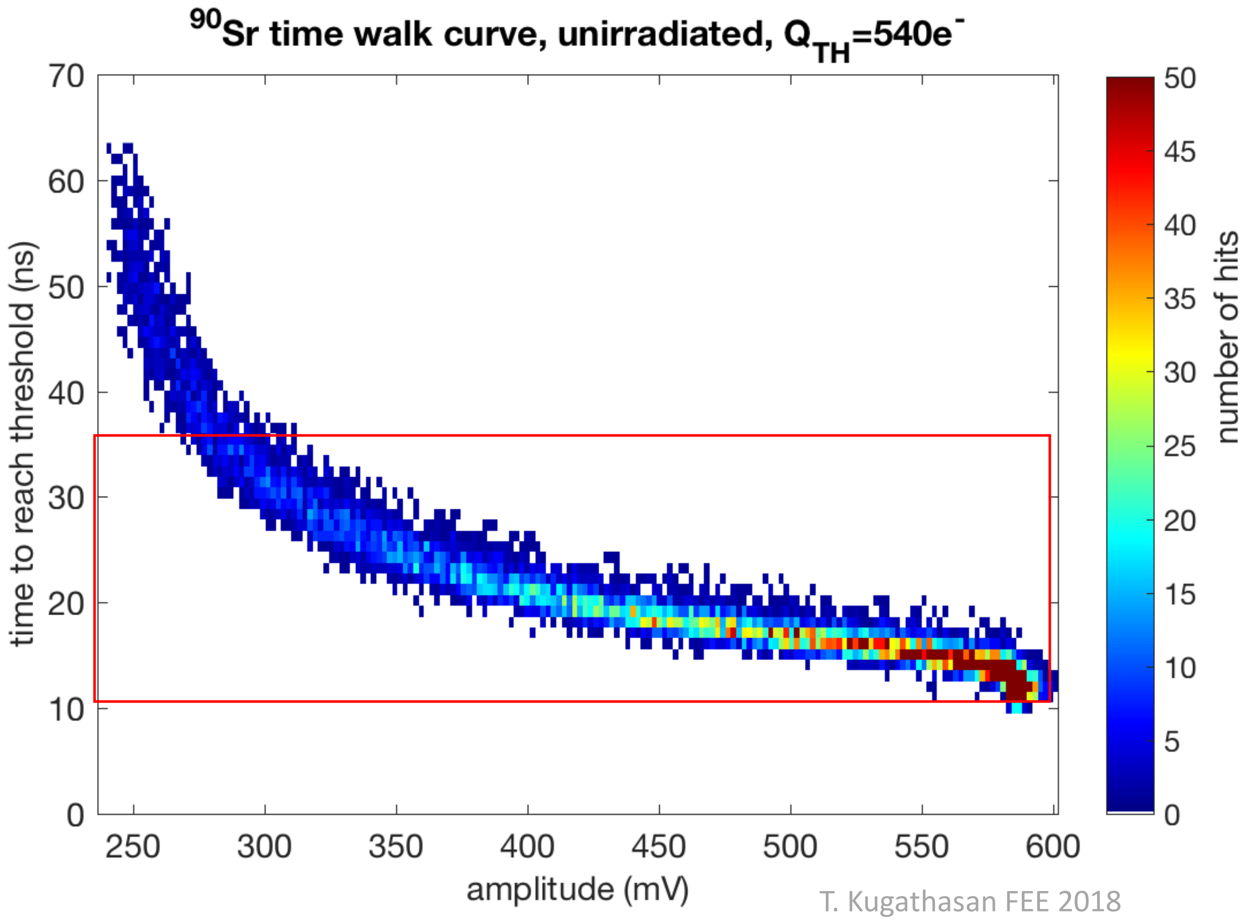

T. Kugathasan FEE 2018

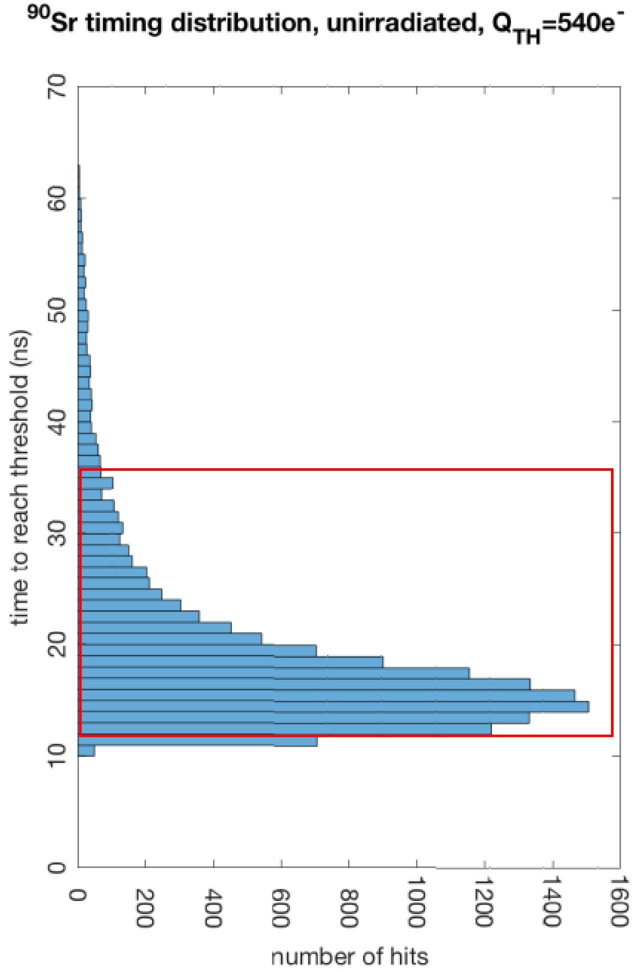

MALTA measurement results

- Charge collection timing remains fast after irradiation to 10^{15} n_{eq}/cm^2

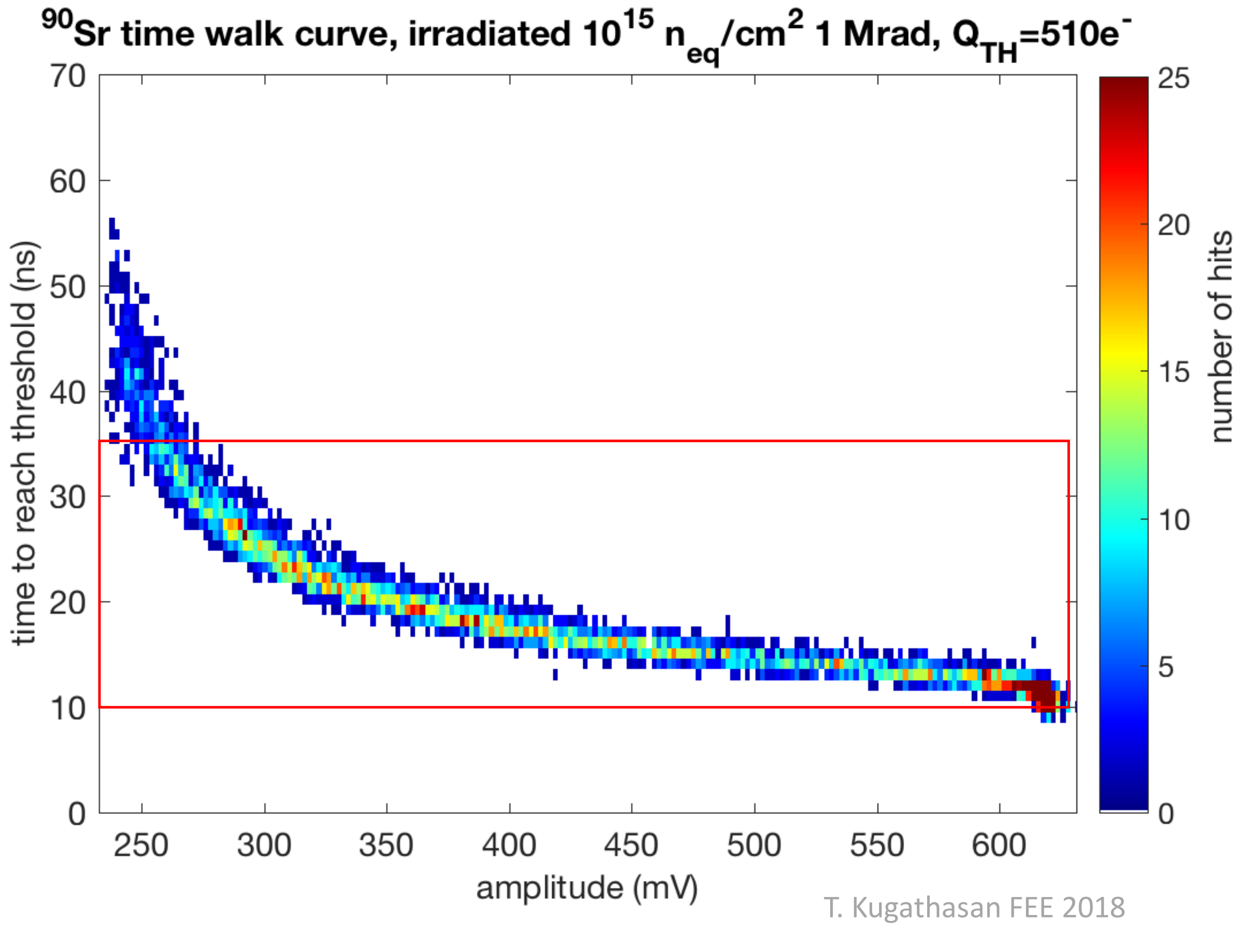

T. Kugathasan FEE 2018

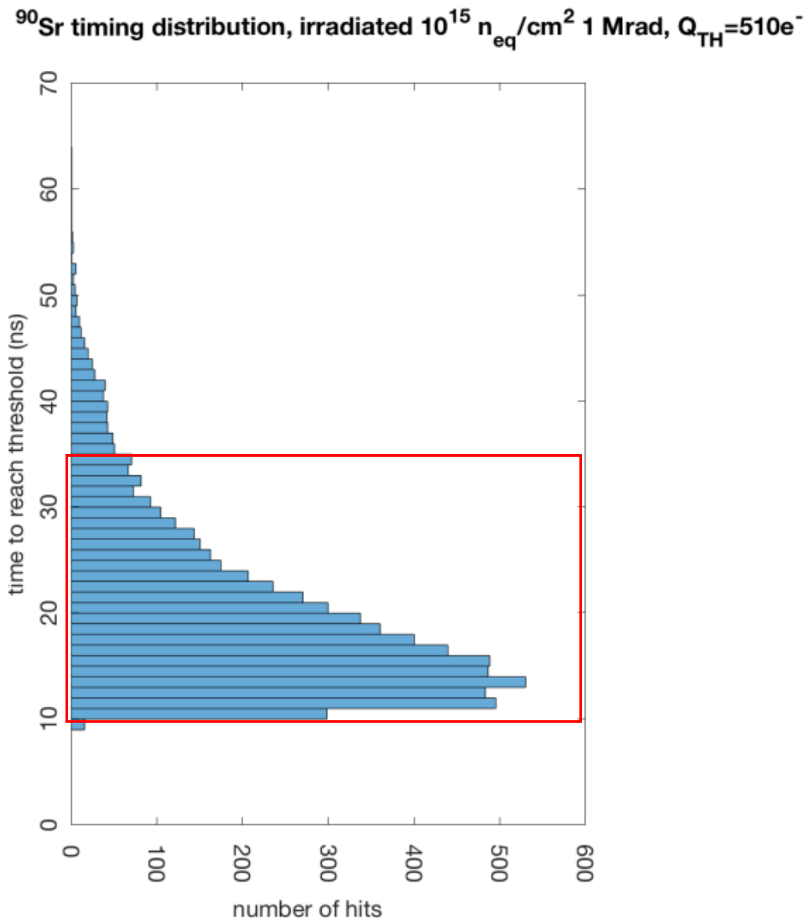

Conclusions & Outlook

A) Conclusion

- DMAPS large scale demonstrator chips were successfully implemented, to prove the feasibility of CMOS DMAPS for the harsh radiation environment of the outer layers of ALTAS ITK
- Two different concepts were tested: Large and small collection electrode
  - Radiation tolerance of the large collection electrode designs is high and the efficiency is >98% after irradiation to 10^{15} n_{eq}/cm^2 (LF-Monopix)
  - The advantage of the small collection electrode design is the very small detector capacitance that leads to low power consumption, low noise and low crosstalk. ENC ≅ 10e, Low total power consumption: ≅ 110mW/cm² (TJ-Monopix, even lower for MALTA due to the asynchronous readout)
  - Increased radiation tolerance is achieved via a process modification. Source tests (^{55}FE and ^{90}Sr) indicate that good spectra and timing after irradiation to 10^{15} n_{eq}/cm^2 are conserved after irradiation, while the electronics remain fully functional

B) Outlook

- Test beam measurement of TJ-Monopix and MALTA took place at ELSA and SPS (ongoing)
- Successful operation and correlation with the ANEMONE telescope (MIMOSA + FEI4)
- Data analysis is ongoing

Thank you!

Backup

- Hardware based on the MIO (multi – input – output board, GPAC (general purpose analog card)
- Both MIO2 and MIO3 are supported
- Firmware and communication and slow control based on the basil framework
- Python based control and data analysis software

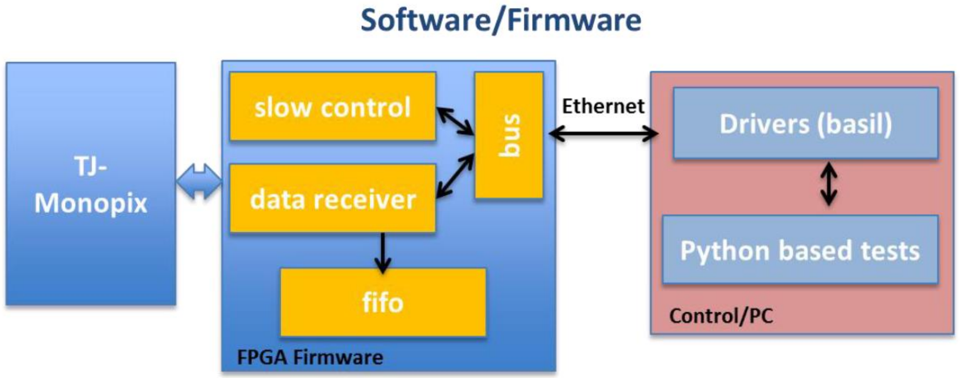

Software available at: https://github.com/SiLab-Bonn/tjmonopix-daq (still under development)

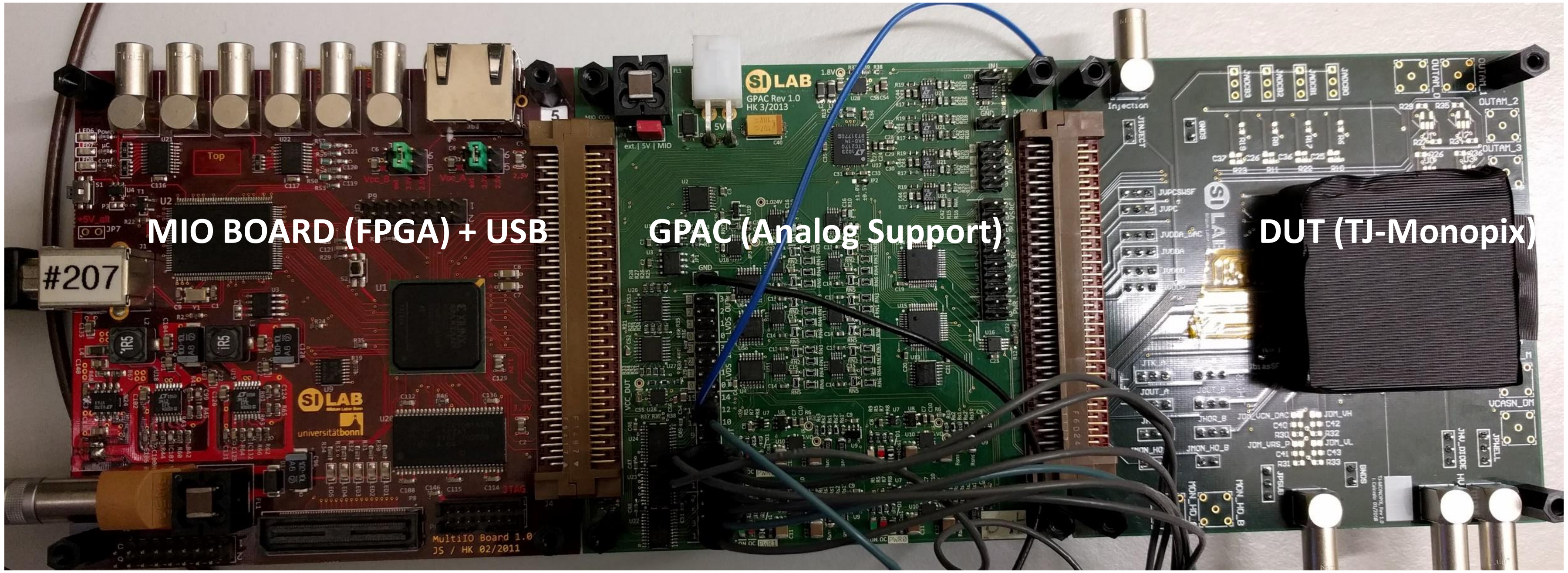

Backup

- It is assumed that in the final prototype
  - 2 double columns per r.o. unit => 512 × 4 pixels
  - 20 MHz column bandwidth: **50 ns** **(2 BC)** per hit readout

    => a simple math: max. allowed hit rate = 1/column bandwidth = **0.5 hit/r.o.unit/BC**
- Inefficiency caused by trig. memory pileup not included here **=>** pure matrix performance
- Data loss increases steeply beyond **600 MHz/cm²** **=> ~ 0.44 hits/r.o.unit/BC**

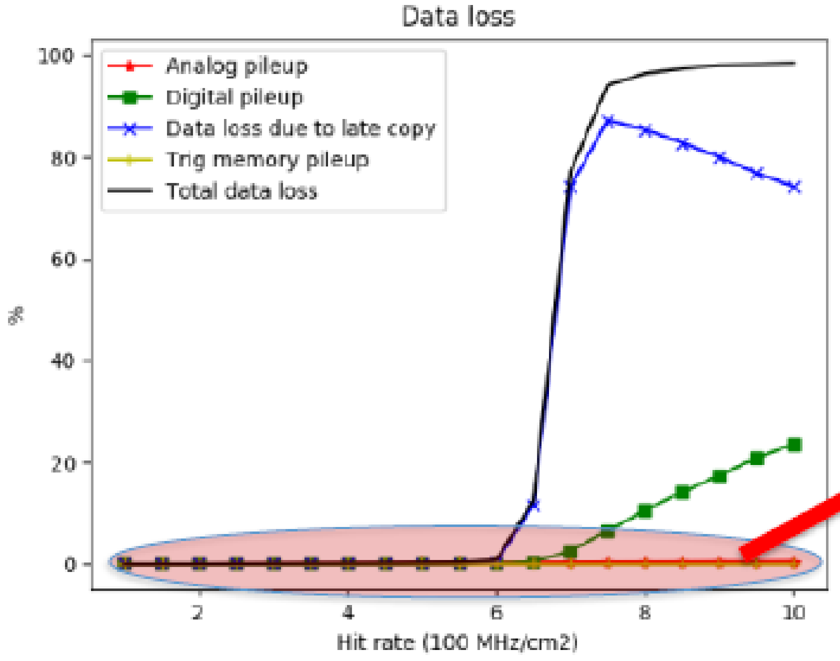

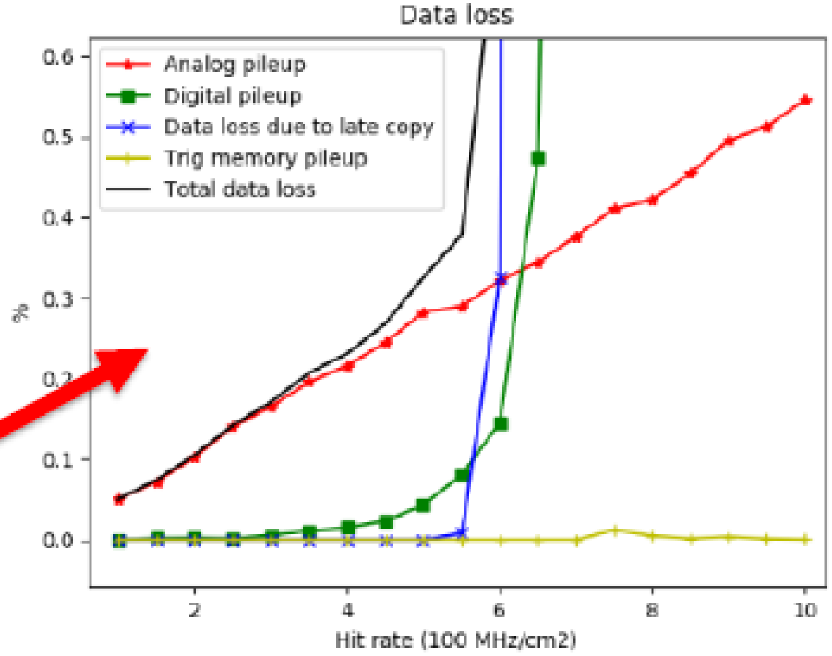

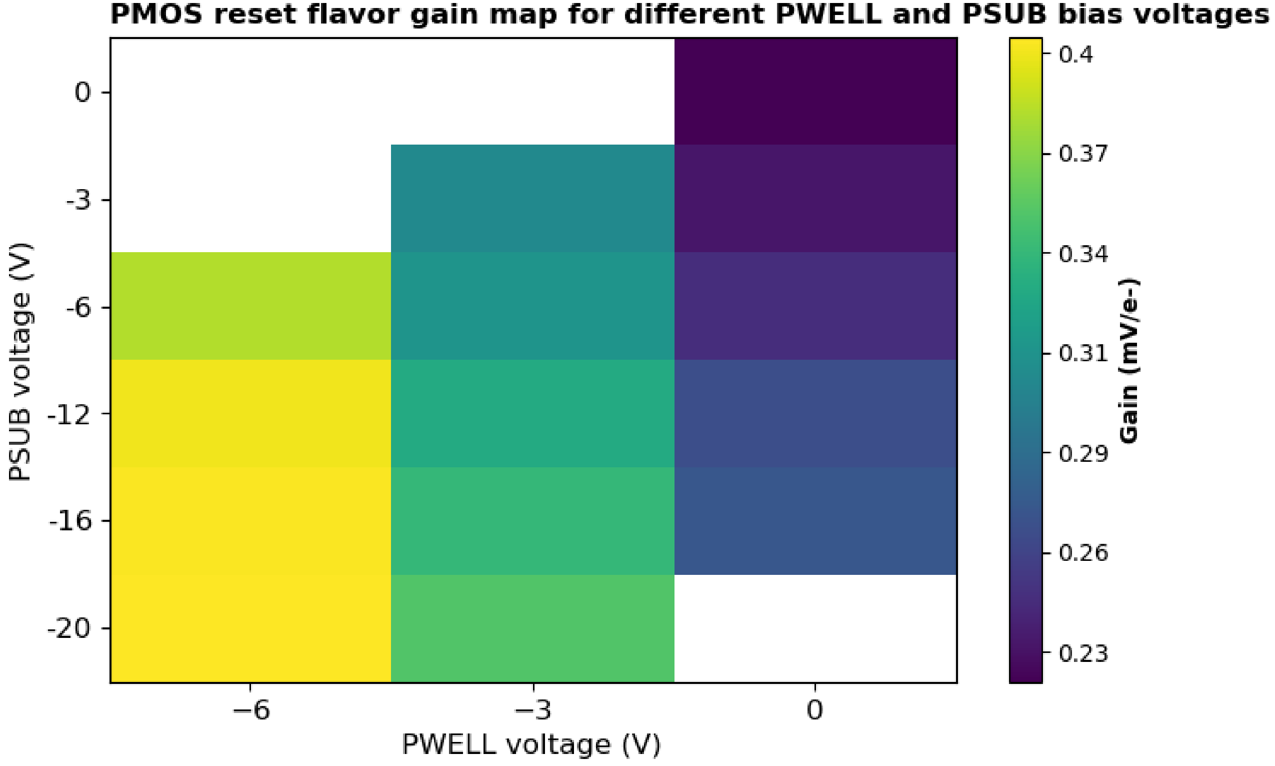
PMOS reset flavor gain map for different PWELL and PSUB bias voltages
PSUB voltage (V)
0
-3
-6
-12
-16
-20
−6
−3
0
PWELL voltage (V)
0.4
0.37
0.34
0.31
0.29
0.26
0.23
Gain (mV/e-)

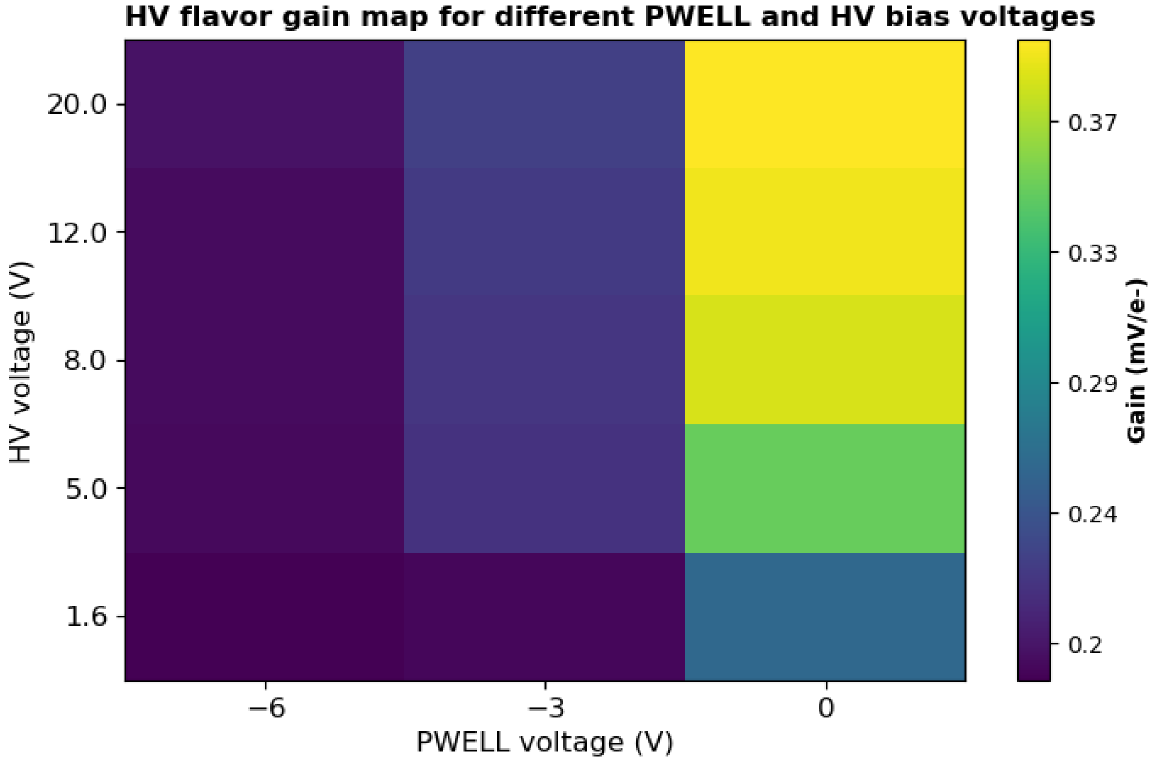
HV flavor gain map for different PWELL and HV bias voltages
HV voltage (V)
20.0
12.0
8.0
5.0
1.6
−6
−3
0
PWELL voltage (V)
0.37
0.33
0.29
0.24
0.2
Gain (mV/e-)

^{90}Sr spectrum: Modified process after irradiation – Investigator chip

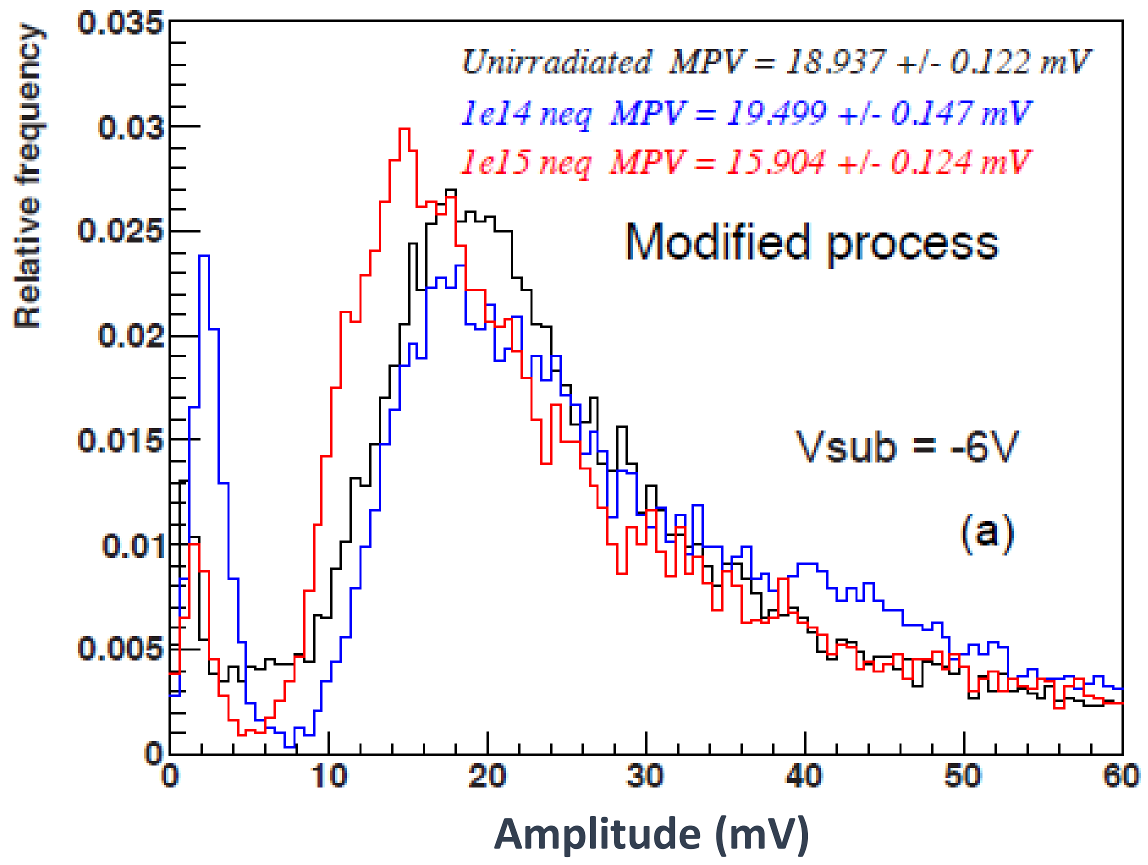

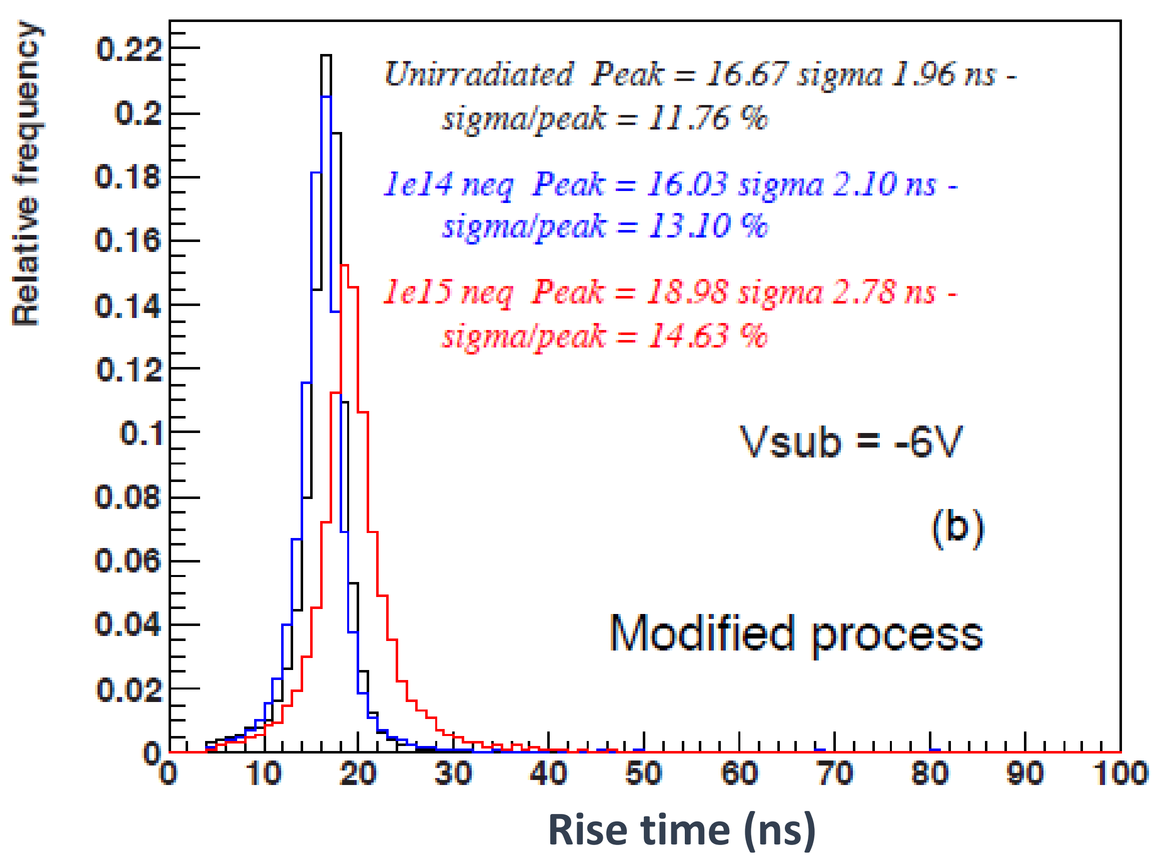

H. Pernegger et al., DOI 10.1088/1748-0221/12/06/P06008

Backup

- **Successful integration with the ANEMONE telescope: 6 MIMOSA26 planes + 1 FEI4 plane for timing**
- **Online monitor functionality implemented**
- **Ongoing data analysis**

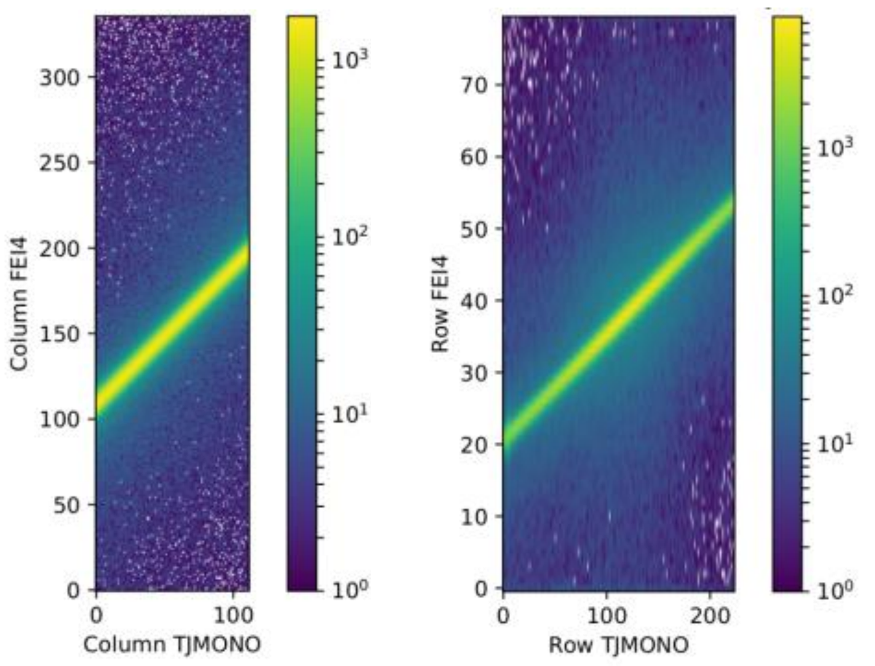

Correlation with the FEI4 timing plane

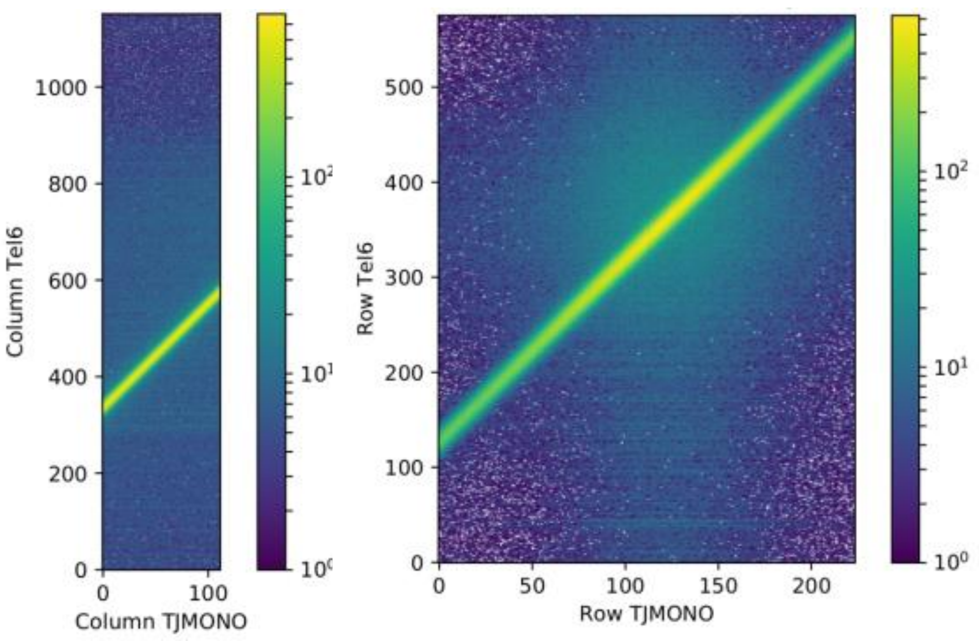

Correlation with the M26 (track reconstruction) planes